

2014

Modeling spacing factor requirements and measuring water permeability in hydrated Portland cement paste

Xinyao Li
Iowa State University

Follow this and additional works at: <https://lib.dr.iastate.edu/etd>



Part of the [Civil Engineering Commons](#)

Recommended Citation

Li, Xinyao, "Modeling spacing factor requirements and measuring water permeability in hydrated Portland cement paste" (2014).
Graduate Theses and Dissertations. 14219.
<https://lib.dr.iastate.edu/etd/14219>

This Thesis is brought to you for free and open access by the Iowa State University Capstones, Theses and Dissertations at Iowa State University Digital Repository. It has been accepted for inclusion in Graduate Theses and Dissertations by an authorized administrator of Iowa State University Digital Repository. For more information, please contact digirep@iastate.edu.

**Modeling spacing factor requirements and measuring water permeability in hydrated
portland cement paste**

by

Xinyao Li

A thesis submitted to the graduate faculty
in partial fulfillment of the requirements for the degree of
MASTER OF SCIENCE

Major: Civil Engineering (Civil Engineering Materials)

Program of Study Committee:
Peter C. Taylor, Co-Major Professor
Kejin Wang, Co-Major Professor
Roy Gu, Co-Major Professor
Mervyn G. Marasinghe

Iowa State University

Ames, Iowa

2014

Copyright © Xinyao Li, 2014. All rights reserved.

TABLE OF CONTENTS

ACKNOWLEDGEMENTS.....	iv
ABSTRACT	v
CHAPTER I. INTRODUCTION.....	1
1.1 Significance of the Project	1
1.2 Thesis Objectives	1
1.3 Thesis Organization	1
CHAPTER II. LITERATURE REVIEW	3
2.1 Durability	3
2.2 Porosity	3
2.2.1 Classification of pores based on size	3
2.2.2 Effects of air voids	4
2.3 Role of Water in Concrete	5
2.4 Water Permeability	6
2.4.1 Water permeability of hardened cement paste:.....	6
2.5 Cold Weather	8
2.5.1 Hydraulic Pressure Theory	8
2.5.2 Osmotic Pressure Theory	9
2.5.3 Energy of Solidification Theory	11
2.6 Existing Water Permeability Measurements.....	12
2.6.1 Autoclave test	12
2.6.2 Germann water permeability test.....	13
2.6.3 Field permeability test (Florida test)-FPT.....	14
Summary	15
References	16
List of Figures	17
List of Tables	17
CHAPTER III. MODELING SPACING FACTOR OF AIR VOIDS REQUIRED FOR HYDRATED PORTLAND CEMENT PASTE	18
Abstract.....	18

3.1 Introduction.....	19
3.1.2 Factors affecting frost resistance of cement paste	19
3.1.2 Purpose of this study	20
3.2 Sensitivity Study on Existing Model	20
3.3 Conclusions.....	34
References.....	35
List of Figures.....	36
List of Tables	36
CHAPTER IV. FALLING HEAD PERMEAMETER FOR MEASURING CEMENT PASTE WATER PERMEABILITY	37
Abstract.....	37
4.1 Introduction.....	38
4.1.1 Permeability of cement paste	38
4.1.2 Approach to challenges.....	40
4.2 Materials and Mix Proportion.....	40
4.3 Testing Procedures.....	42
4.4 Results and Discussion	44
4.4.1 Sources of error.....	44
4.4.2 Water permeability calculation	49
4.5 Conclusions.....	53
References.....	54
List of Figures	55
List of Tables	55
CHAPTER V. CONCLUSIONS	56
APPENDIX A. STATISTIC ANALYSIS FOR WATER PERMEABILITY ESTIMATION	58
APPENDIX B. VIEWS OF WATER PERMEAMETER	63

ACKNOWLEDGEMENTS

I would like to thank my supervisors, Drs. Peter C. Taylor, Kejin Wang, and Roy Gu, who have been tremendous mentors for me. I feel motivated and encouraged every time I attend their meetings. The useful comments, remarks, and engagement through the learning process of this Master's thesis have been priceless for these two years. Without their supervision and constant help, this thesis would not have been possible.

I would like to thank my committee member, Dr. Mervyn G. Marasinghe, for serving as my committee member. Also, I want to thank him for allowing my defense be an enjoyable moment, and for his brilliant comments and suggestions in statistical analysis, thank you.

Furthermore, I would like to acknowledge with much appreciation the crucial role of Portland Cement Concrete lab manager, Robert F. Steffes, who gave permission to use all required equipment and the necessary materials to complete the task. He provided continuous technical support for the apparatus' modification. I would like to express the deepest appreciation to him.

Finally, a special thanks to my family. Words cannot express how grateful I am to my grandmother, grandfather, my mother, father, and my husband for all of their supports. Your prayers for me are what have sustained me thus far. I would also like to thank all of my friends, who supported me in writing this thesis and provided me with incentives to strive towards my goal.

ABSTRACT

Small, well-dispersed air voids in hydrated cement paste can improve workability, reduce bleeding and segregation, and improve resistance to freezing and thawing. To characterize the air void system in cement paste, not only the amount and size of air voids are important, but their distribution (spacing factor) is also significant. This thesis investigates the frost action mechanism in cement paste and how the spacing factor closely relates with it. Also, this thesis provides detailed information about testing the cement paste's water permeability by using a falling head permeameter on saturated samples.

Paper one is a sensitivity study from an existing modeling system for determination of maximum spacing factors. Conclusions are drawn by analyzing the existing mathematic model and comparing the theoretic values with experimental values.

Paper two describes work conducted in the development of a method to test water permeability of saturated hydrated cement paste. This is a cost effective method to test the water permeability, since the work is achieved by revising of existing Ballim oxygen test. From test results and observations, several apparatus' revisions have been completed. Some recommendations are provided for further improvement of the test apparatus.

CHAPTER I. INTRODUCTION

1.1 Significance of the Project

This study seeks to better understand the air void system required to protect concrete from freezing action based on modelling. Besides, the sensitivity study of a required spacing factor for water in capillary pores during freezing, the work illustrates the influence of different critical factors. Permeability is one of the dominant factors that influence the required spacing factor. For this reason, laboratory tests for water permeability of cement paste have been conducted using a water permeameter developed from the Ballim oxygen test.

1.2 Thesis Objectives

This thesis addresses three objectives. They include;

1. The flow of water through cement paste is caused by pressure resisted by impermeability. By using models to determine flow for a given pressure and impermeability in a porous medium, the distance a drop of water under given conditions can be found.
2. Assess the maximum spacing factor required to protect concrete from freezing action by modelling the movement of freezing water in a porous medium.
3. Investigate the feasibility of modifying an existing air permeameter to conduct water permeability tests on saturated paste samples.

1.3 Thesis Organization

This thesis is divided into six chapters. Chapter 1 provides a general introduction.

Chapter 2 gives a brief literature review of concrete and hydrated cement paste durability, pores, water permeability, and frost action. The purpose of this review is to provide background

and general information about durability, especially about frost resistance ability related with the air void system in concrete and hydrated cement paste.

Chapters 3 and 4 are technical that discuss the work conducted

Chapter 5 provides conclusions and recommendations for future research and industrial application.

CHAPTER II. LITERATURE REVIEW

2.1 Durability

Durability of portland cement concrete (according to ACI Committee 201) is the ability to resist deterioration such as weathering action (frost action or fire), cracking happens from crystallization of salts in pores chemical attack, and abrasion. As long as the microstructure of concrete interacts with environment, its properties will change. If it can retain its quality when exposed to its intended service environment for the intended service life, it can be counted as durable concrete [1].

Since water can penetrate into permeable concrete, it becomes the agent for destruction of concrete. The primary types of concrete deterioration include the corrosion of reinforced steel, exposure to cycles of freezing and thawing, alkali-silica reaction, and chemical attack [2].

Since permeability of concrete controls the rate of solution transport through connected pores, this study focuses on the influences of pores and permeability on concrete durability.

2.2 Porosity

2.2.1 Classification of pores based on size

Mehta and Monteiro [1] put pores into three categories: interlayer space in C-S-H, capillary voids, and air voids.

Pores in the interlayer space in C-S-H are the smallest at a nanometer scale. Because of their size, these voids have little impact on the strength and permeability of hydrated cement paste. Their effects on drying shrinkage and creep are controlled by removal of water held by hydrogen bonding, which will only occur at very low humidity levels.

Capillary voids are the space not filled by the hydration products, and are in the range of 10 nm to 5 μm [3]. The pore size distribution is determined by the water-to-cement ratio and

degree of cement hydration [4]. Higher water-to-cement ratio leads to an increase in the volume and size of capillary voids. With continued hydration, there is a reduction in permeability and an increase in strength.

As a result of mixing and placing, air is always present in concrete mixes. Air is trapped in fresh concrete intentionally or unintentionally in the form of gas bubbles surrounded by a thin liquid film. These bubbles vary in size and shape in hardened concrete. There are two types of air voids: entrapped air voids and entrained air voids. Voids larger than about 1 mm in diameter and that are irregularly shaped are considered entrapped, and a purpose of vibration is to remove them. Smaller, spherical voids that are stabilized through use of chemicals are entrained air voids [1].

Each air void is considered to provide protection from freezing and thawing in a spherical zone somewhat larger than the size of the void. It is therefore desirable to have a large number of small voids close together so that their areas of influence overlap and so that all of the paste is protected. Typically, it is assumed that an average spacing between voids of about 200 μm will provide adequate protection. This translates to a total volume of air voids of about 18% to 20% of the cement paste volume, or 4% to 7% of concrete volume in conventional systems [5]. One of the aims of this work is to verify through modelling that this value is still reasonable, considering that it was developed using mixture ingredients that are significantly different from those in current use.

2.2.2 Effects of air voids

Large voids are generally detrimental to hardened concrete because they increase permeability and reduce strength, so their removal is necessary. However, workability is improved when the air void system is in the form of small and well-dispersed bubbles. They act

as cushions between aggregate particles, reducing friction and interlocking. For a given total air content some of the loss in the strength can be offset by the reduction in water requirement [5]. Moreover, air voids also reportedly reduce bleeding and segregation.

The most important effect of air voids is to release the pressure exerted by ice expansion as pore-water freezes in the capillaries. In addition, dissolved salts in the pore water exert osmotic pressure during freezing. Since water travels from the gel pores to capillary pores, which from the ions less concentrated site to more concentrated site, this movement of water equalize the solution concentration and generate pressure at capillary pores.

The mechanism of how air voids system protects hardened cement paste is to release pressure by providing a place for expanding pore solution to move into. The air bubbles have to be distributed in such a way that expanding fluid can reach the void before it freezes.

Traditionally, air content in concrete, expressed as a percentage of concrete volume, is the only characteristic of air voids system that has been measured. This meant that quality control could be based solely on air content. However, with new admixtures on the market this assumption is no longer necessarily valid because the size distribution of voids varies, making it necessary to review critical spacing factors, and how to measure them.

2.3 Role of Water in Concrete

The role of water in concrete at the time of mixing is to lubricate the mixture and provide workability. For most aggregate systems more water is required for this purpose than is needed to hydrate the cement. Water is also a necessary ingredient for cement hydration [1]. When the concrete is exposed to drying conditions, evaporable water (that includes all the capillary water and some of the adsorbed water) leaves concrete. The speed of this process and amount of evaporable water lost are affected by the ambient conditions and the thickness of a concrete

element [1]. Water content influence pores in cement paste by affecting volume of hydration products. After water has been consumed by cement hydration reaction or by evaporation to the environment, the unfilled space is pores in cement paste. The volume of mixing water directly affects the permeability of cement paste. In general, lower permeability is related with greater durability [6].

2.4 Water Permeability

2.4.1 Water permeability of hardened cement paste:

The rate of deterioration of cement paste is strongly influenced by the ease with which fluids can penetrate the matrix, which in turn is controlled by the connectivity and volume of the capillary pores. “Permeability is defined as the property that governs the rate of flow of a fluid in to a porous solid.” [1] Therefore, permeability is an indicator of the degree of interconnection of pores in concrete [3]. For a steady-state flow, the coefficient of permeability (K) is determined from

Darcy’s expression:

$$\frac{dq}{dt} = K \frac{\Delta H A}{L \mu}$$

Where dq/dt =rate of fluid flow

μ =viscosity of the fluid

ΔH =pressure gradient

A=surface area

L=thickness of the solid

The coefficient of permeability will therefore decrease with continued hydration. As shown in Table 1 and Table 2, because the porosity of hydrating cement paste decreases with

increasing hydration. Although there is no direct relationship between porosity and coefficient of permeability, the latter drops a large amount once the former decreases to about 30 percent.

Table 1. Reduction in permeability of a 0.7 w/c cement paste with the progress of hydration [1]

Age days	Coefficient of Permeability (m/s $\times 10^{-13}$)
Fresh	20,000,000
5	4,000
6	1,000
8	400
13	50
24	10
Ultimate	6

Table 2. Reduction of permeability by cement hydration of w/c= 0.5 [7]

Coefficient of Permeability (m/s)	
Fresh	Ultimate
5.6×10^{-7}	4.4×10^{-14}
6.3×10^{-7}	5.2×10^{-14}
5.1×10^{-7}	5.7×10^{-14}
8.4×10^{-7}	6.3×10^{-14}

2.5 Cold Weather

The effects of freezing and thawing, and deicing salts are a major problem for concrete structures in cold climates. There are several forms of frost damage. Cracking and spalling are common, caused by moisture freezing inside cement paste, which leads to progressive expansion of the cement paste during freezing and thawing cycles. Scaling is another form of frost damage for concrete slabs once exposed to moisture and deicing salts. Also the cracking of coarse aggregate during freezing and thawing cycles is known as D-cracking, which occurs parallel to joints and edges.

There are three theories discussed in the literature to explain the effects of frost action in concrete.

2.5.1 Hydraulic Pressure Theory

Powers described the mechanisms of frost action and effectiveness of air entrainment in cement paste as follows: The frozen water in capillary pores expands 9 percent during freezing, the volume increase results in the dilation of the capillary pores or forcing the excess water moves to the nearest “escape boundary”. Both effects can happen at the same time. Hydraulic pressure is developed during this process, and its magnitude is determined by the “distance to an escape boundary, the permeability of the intervening materials and the rate at which ice is formed” [8]. In this theory, the escape boundary for every capillary cavity in the paste should not be further than $76\mu\text{m}$ to $102\mu\text{m}$ by using proper air-entraining agent, otherwise, the disruptive pressure will be generated in saturated cement paste [8].

The required pressure to force water to move a certain distance can be calculated by Darcy’s law of water flow through a porous body. Once the tensile strength of the cement paste cannot carry the hydraulic pressure, cracks will occur. There are three factors related to the

magnitude of pressure: the distance to the nearest air-filled void, the permeability of the cement paste, and the cooling rate [9]. The half distance between two air-filled voids is the air void spacing factor. The air void spacing factor should be small enough for the hydraulic pressure to remain below the tensile strength under given freezing conditions [9].

Air voids of the size desirable for frost protection are unstable in normal conditions, therefore it is necessary to use air entraining agents to stabilize them. As for the permeability of cement paste, if the permeability is higher, the pressure will be lower. At the same time, higher permeability and porosity will make the volume of air voids system increase, so that the ice will fill more volume before forcing water to travel. The last factor have influence on the magnitude of pressure is cooling rate, which according to Powers [8] affects the rate of pressure build up. A smaller spacing factor is required to accommodate increasing cooling rate.

For the hydraulic pressure theory, there is a mathematical model describing the relationship among cement paste properties, safe traveling distance, and freezing rate. In this theory, it assumes that water travels away from the frozen sites during freezing, which is different than the osmotic pressure theory that will be discussed next.

2.5.2 Osmotic Pressure Theory

Together with Helmut, Powers discovered that water traveled toward frozen sites, which is opposite to hydraulic pressure theory. Because capillary pores are not filled with pure water, water will travel from gel pores where ions are less concentrated to capillary pores (frozen site), which is osmic movement. In the pore solution, it contains alkalis, calcium, hydroxyls, and chlorides (if salts are included) [9].

Through a simple test, the osmotic pressure theory can be illustrated as the following figure 1 [10]. A funnel with water permeable membrane at the bottom is partially filled a with

high-concentration solution. The membrane only allows the water to pass through but prevents movement of solutes. Then submerge the funnel in the pure water. At this time, the height of solution in the funnel is at the same height of the water level surrounding the funnel. After a while, it can be observed that the height of solution will be raised since pure water has passed through the membrane.

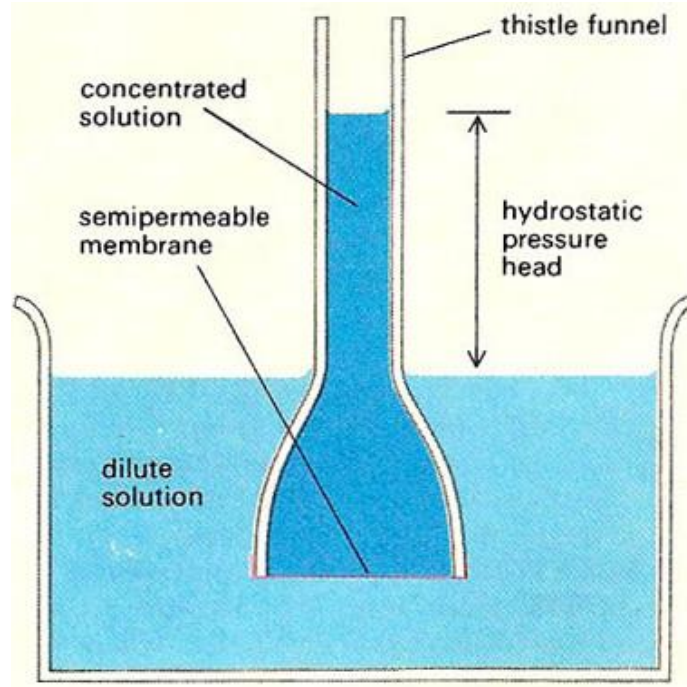


Figure 1. Osmotic pressure

Another effect of ions in the pore solution of cement paste is that they lower the freezing point of the pore solution. Once the freezing point is reached, pure water will transform to ice, while leaving ions in the remaining liquid solution. Because of the higher concentration of ions in the solution, the freezing point then drops; so stopping the continuation formation of ice crystals. The freezing temperature also depends on the size of pore. At the smaller pores (gel pores), water cannot freeze at temperatures above -78°C [11]. The solution at gel pores is less diluted than the frozen site, which causes water traveling to high-concentrated solution (frozen site). After water removed from these smaller pores, shrinkage of cement paste is the

consequence. When temperature keeps dropping, ice crystal keeps growing and penetrates the air void. High-concentrated solution at the frozen site is lowered once the less diluted solution arrived. This process leads to higher freezing point that leads to more ice formation and builds stresses around the frozen site. The osmotic pressure theory is the first model to demonstrate the scaling on concrete surface with the present of deicing salts [9].

In order to protect capillary (small pores), the entrained air voids plays the role to attract the travelling solution [12]. The air-filled voids can offer more room for water expansion. Besides, solution at smaller, less-diluted pores will move towards frozen site includes both capillary and entrained air voids. The same as hydraulic pressure theory, the space distance between air voids is relatively small enough, the solutions will be attracted to these sites, which is the way to prevent extra stress development.

2.5.3 Energy of Solidification Theory

Energy of solidification theory is discovered by Powers and Helmuth [12] in the early 1950s. They found cement paste specimens with air entrainment contracted during freezing, which contradicts the hydraulic pressure theory indicating expansion. The contraction of cement paste is the effect of pore water, pore size distribution, and free-energy equilibrium [12]. For the reason of freezing point can be lowering by high surface tension, ice crystals will firstly form in capillary voids comparing to gel pores. Comparing with the gel pores with liquid water, the ice nucleation in the capillary voids leads to a lower free-energy state. Thermodynamically, the liquid water will travel towards the capillary voids to create equilibrium. Once the unfrozen water reaches the capillary voids, it will form ice crystals and cause expansion to crack cement paste. Contraction (shrinkage) of cement paste happens at the same time as rigidly held gel pore water traveling to air voids through capillary voids.

With the use of air entraining agent, the entrained air voids will provide sites for unfrozen water to travel to. In this way, the damage of cement paste will be reduced since there is plenty of space for ice expansion.

Another explanation for the contraction of cement paste is provided by Litvan [13]. In his theory, the contraction is caused by unequal vapor between the external ice and the unfrozen water in the gel pores. With the decreasing of temperature, more percentage of liquid water are turning into the solid ice state than the reverse way. It illustrates that vapor pressure of ice drops faster than that of water, which leads the gel pore water to move to the external ice and it is the cause of shrinkage in cement paste.

The role of air void is not the same the hydraulic pressure theory and osmotic pressure theories. However, all three theories benefit from the entrained air void system. According to Litvan [13], during water freezing, it can provide reservoir the expelled water can travel to before water must travel to an external surface.

2.6 Existing Water Permeability Measurements

2.6.1 Autoclam test (Basheer, 1993)

The autoclam test is used for measuring the air permeability, unsaturated water permeability and water absorption into near surface zone of porous materials, both in laboratory and on site [14]. The schematic set up is shown in Figure 2. There are two components of the autoclam, the autoclam body and its electronic controller and data recording system [14]. For the water permeability test, the test chamber is filled with water, then by providing a constant pressure of 50kPa by a stepper motor moving a piston, the water penetrates into capillary pores. With the constant pressure, volume of water delivered is recorded and the rate of flow can be used to describe water permeability. However, the limitation for autoclam test is the moisture

state of concrete influences the rate of flow. Since the intention for this test is to measure the near surface zone, the water penetrates into concrete through surface, then the moisture state of concrete varies by depth. It is difficult to reach a constant moisture state, especially when the concrete slab is thick, then the measurement of water permeability is not reliable.

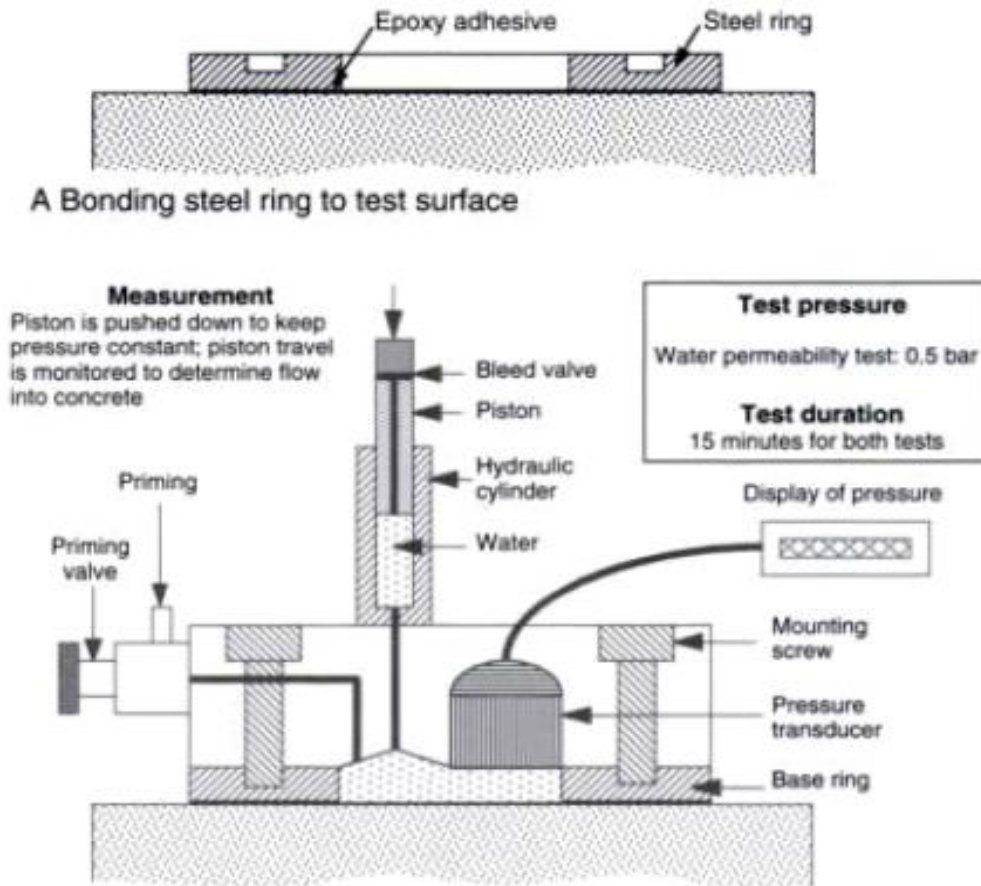


Figure 2. Schematic setup of autoclam test for water permeability measurement [15]

2.6.2 Germann water permeability test (Germann Instruments, Inc. 2009)

Germann water permeability test was invented for on-site measurement of skin-concrete in finished structures under an applied water pressure [16]. Figure 3 is the schematic illustration of the GWT setup. The pressure chamber tightly attached to the surface of concrete by two anchored clamping plier. By pushing a piston into chamber, water permeates into concrete under

the desired constant pressure. The distance of piston travels for certain time period is recorded, then the permeability of concrete can be calculated. The major drawback for this instrument is rate of water evaporation from surface of clamping plier's outer edge into air is not negligible.

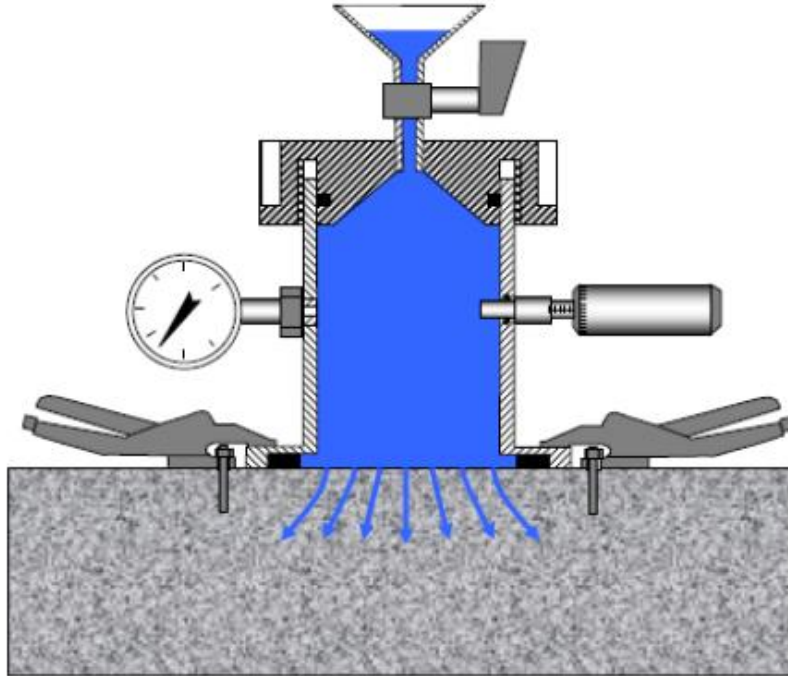


Figure 3. Schematic illustration of the GWT setup [15]

2.6.3 Field permeability test (Florida test)-FPT (Meletiou, Tia, and Bloomquist in 1990s)

This method is conducted by drilling a hole (23mm in diameter and 152mm deep into the concrete) [15] as seen on Figure 4. Water pressurized by a nitrogen bottle penetrates into concrete in the radial direction through the central perforated sleeve. After a steady-state flow is reached, the rate of water flow is recorded under pressure in the range of 10 to 35 bar [15]. Based on the rate of water flow, water permeability can be calculated. The limitation of this test is the direction for water flow into concrete is nonlinear. Besides, this is a destructive method which is not suitable for some cases.

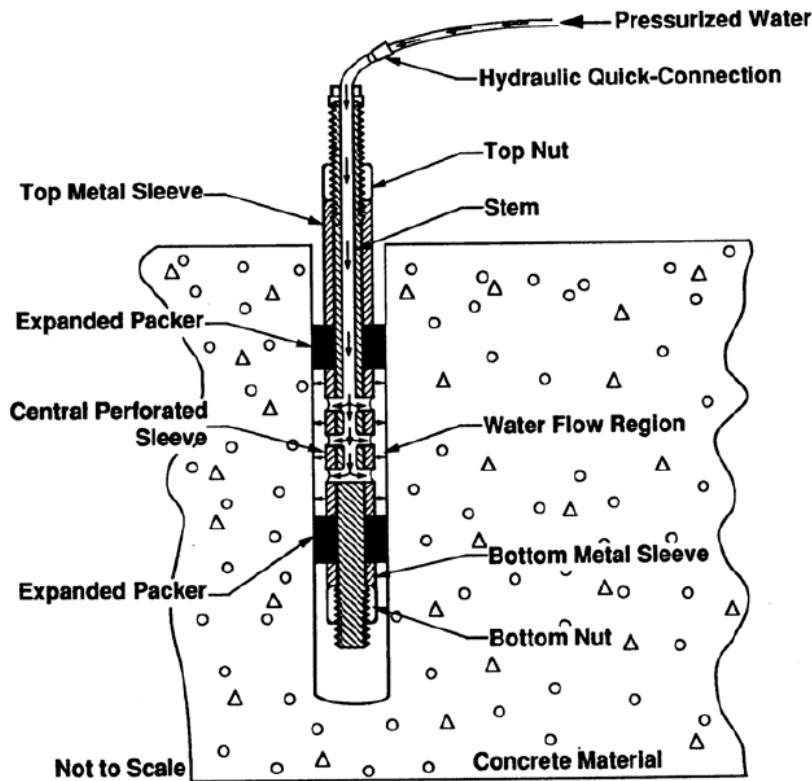


Figure 4. Schematic view of the Florida test setup [15]

Summary

By illustrating the influence of pores, water permeability on the ability of cement paste to resist cold weather, the significance of spacing factor, or travel distance to an escape boundary during freezing is demonstrated. Relatively small, well dispersed voids are the key to prevent cement paste from detrimental cracking during freezing and thawing cycles. Work in this project demonstrates how spacing factor is affected by factors like ice formation rate, permeability, and some other characters of the specimen of cement paste and the magnitude of each factor.

References

- [1] P. Kumar Mehta, Paulo J.M. Monteiro, Concrete Microstructure, Properties, and Materials, Department of Civil and Environmental Engineering: McGraw-Hill, 2006.
- [2] "Penetron, Total Concrete Protection, Internal Waterproofing for Concrete," March 2010. [Online]. Available: <http://www.penetron.com/newsletter/mar10-en.htm>. [Accessed 10 11 2013].
- [3] Y. Ballim, "A low cost, falling head permeameter for measuring concrete gas permeability," *Concrete Beton*, p. 13, November 1991.
- [4] A. M. Neville, Properties of concrete, New York, 1996, p. 844.
- [5] K. Hover, "Why is there air in concrete," *Concrete Construction*, 1993.
- [6] D. Burden, "The durability of concrete containing high levels of fly ash," PCA, Skokie, 2006.
- [7] T. C. Powers, L. E. Copeland, J. C. Hayes, H. M. Mann, "Permeability of Portland Cement Paste," *Journal of the American Concrete Institute*, vol. 51, p. 285, April 1955.
- [8] T. C. Power, "The Physical Structure and Engineering Properties of Concrete," *Portland Cement Association*, vol. Bulletin 90, 1958.
- [9] C. C. Jr., Microscopic Observations of Internal Frost Damage and Salt Scaling, University of California, Berkeley: UMI Dissertations Publishing, 2008.
- [10] F. P. Glasser, "Thermodynamics of Cement Hydration," *Materials Science of Concrete VII*, 2005.
- [11] Jussara Tanesi and Richard Meininger, "Freeze-thaw resistance of concrete with marginal air content," December 2006.
- [12] T. C. Powers, R. A. Helmuth, "Theory of Volume Changes in Hardened Portland-Cement Paste During Freezing," *Highway Research Board*, p. 32, 1953.
- [13] G. G. Litvan, "Adsorption System at Temperatures Below Freezing-Point of Adsorptive," *Advances in Colloid and Interface Science*, vol. 9, no. 4, pp. 253-302, 1978.
- [14] "Autoclam," Amphora NDT, 2012-2014. [Online]. Available: <http://www.amphorandt.com/autoclam.html#Overview>. [Accessed 3 2 2014].
- [15] Javier Castro, Robert Sprag, Phil Compare, William Jason Weiss, "Portland and cement concrete pavement permeability performance," INDOT Research, 2010.

List of Figures

Figure 1. Osmotic pressure	10
Figure 2. Schematic setup of autoclam test for water permeability measurement [15].....	13
Figure 3. Schematic illustration of the GWT setup [15].....	14
Figure 4. Schematic view of the Florida test setup [15]	15

List of Tables

Table 1. Reduction in permeability of a 0.7 w/c cement paste with the progress of hydration.....	7
Table 2. Reduction of permeability by cement hydration of w/c= 0.5 [7].....	7

CHAPTER III. MODELING SPACING FACTOR OF AIR VOIDS REQUIRED FOR
HYDRATED PORTLAND CEMENT PASTE

A Paper to be submitted to Transportation Research Board

Xinyao Li¹, Peter C. Taylor², and Kejin Wang³

Abstract

The expansion of ice and the rapid movement of unfrozen water pushed ahead of the growing ice crystals causes stress in the cement paste until it cracks. Sufficient and well distributed air voids in the cement paste can cut the flow path, provide spaces for ice to grow, and release the pressure, and prevent the paste from freezing-thawing damage. In the present study, sensitivity study has been conducted to investigate the maximum spacing factor with existing Power's model. In this model, maximum spacing factor is influenced several parameters as degree of saturation, rate of ice formation, and permeability. By selecting the proper parameters, the maximum spacing factor can be determined. To prevent damage, the air voids should be closer than a critical distance which is estimated to be around 210 μm , which is in accordance with experimental work conducted in the 50's [1].

Keywords: cement paste, freezing-thawing damage, permeability, air void, spacing factor

¹ Graduate Student, Iowa State University, Civil, Construction and Environmental Engineering, 136 Town Engineering, Ames, IA 50011, Tel: 515-817-3012, Email: xli@iastate.edu

² Director II, National Concrete Pavement Technology Center, Iowa State University, Ames, IA 50011, Tel: 515-294-9333, Email: ptaylor@iastate.edu

³ Professor, Iowa State University, Civil, Construction and Environmental Engineering, 492 Town Engineering, Ames, IA 50011, Tel: 515-294-5126, Fax: 515-294-8216, Email: kejinw@iastate.edu

3.1 Introduction

In cold weather areas, freeze-thaw durability of cement paste is a critical design parameter. Since hydraulic pressure built up during water freezing, cement paste can be damaged once pressures exceed cement paste's ability to carry them.

3.1.1 Mechanics of water flow in capillary pores during freezing

The process of water freezing in a capillary cavity requires the cavity to dilate by 9% to equal the volume increase of the frozen water. Otherwise, the pressure forces the excess water through the boundaries of the specimen. For most cases, these two effects occur simultaneously. Ice crystals grow in capillary pores, they will damage the cement paste by pushing the capillary walls and generating hydraulic pressure [2]. The expansion of these crystal matrices leads to cracking and loss of stiffness for hydrated cement paste, this is known as frost damage. An empty air void serves as an effective escape boundary to reduce this pressure.

3.1.2 Factors affecting frost resistance of cement paste

Several factors affect frost resistance of cement paste. The first factor is the utilization of air entrainment. Air entraining admixtures are used to provide stable small air voids that are well-dispersed. If an air entrainment agent is properly used, it can provide bubbles spaced at about 0.1 to 0.2 mm in the hardened cement paste to reduce the risk of frost damage [3]. A second factor is the water-to-cement ratio. An increase in water-to-cement ratio leads to decrease the tensile strength of cement paste to carry the hydraulic pressure that is caused by freeze-thaw cycles. Increased w/c will also increase the volume of pores likely to contain water that needs to be accommodated. This means that cement paste with a higher water-to-cement ratio increases the probability of frost damage. A third factor is curing. Proper curing can promote hydration of the cementitious system so reducing permeability and increasing strength. This means moist

curing can improve the ability of cement paste for frost resistance. The fourth factor contributing to frost resistance is the degree of saturation. Normally, damage from frost increases as the degree of saturation increases. This explains the phenomenon that dry or partially dry cement paste does not have the problem of frost damage. However, if the degree of saturation is too high, which means exceeding the critical value, the cement paste will likely crack or spall when exposed to very low temperatures [3].

3.1.2 Purpose of this study

The release of hydraulic pressure depends upon the distance to an “escape boundary”, the permeability of the concrete, and the rate at which ice is formed [4]. In this paper, the emphasis is on determination of safe travel distance. Only when the “escape boundaries” are sufficiently closely spaced, can the cement paste be frost resistant. By performing a sensitivity study of an existing model, the recommended spacing factor is determined.

3.2 Sensitivity Study on Existing Model

The spacing factor for the hardened cement paste air void system can be estimated in freeze-thaw environments [5]. As described by Powers, experience has shown disruptive pressures will develop in a saturated cement paste, once the distance between the nearest escape boundaries (entrained air voids) is larger than 3 to 4×10^{-3} inch. However, there is no clear dividing line for most concrete specifications, since factor like the choice of aggregate comes into play.

Because frost resistance in any hydrated cement paste depends upon the characteristics of the air-void system, tensile strength, degree of saturation, curing history, and rate of freezing [5],

Powers developed a hypothesis for internal frost deterioration of air-entrained concrete, based on hydraulic pressure theory. As shown in Figure 1, the maximum hydraulic pressure existing at the outer boundary of a cement paste shell with radius r_m will rise during ice formation, when water is expelled from the pore [6]. r_b is the radius for the entrained air void in the range of 100-400 μm . \bar{L} is the spacing factor expressed as $r_m - r_b$. In an actual system, ASTM C457 [7] determines the spacing factor through microscopic evaluation.

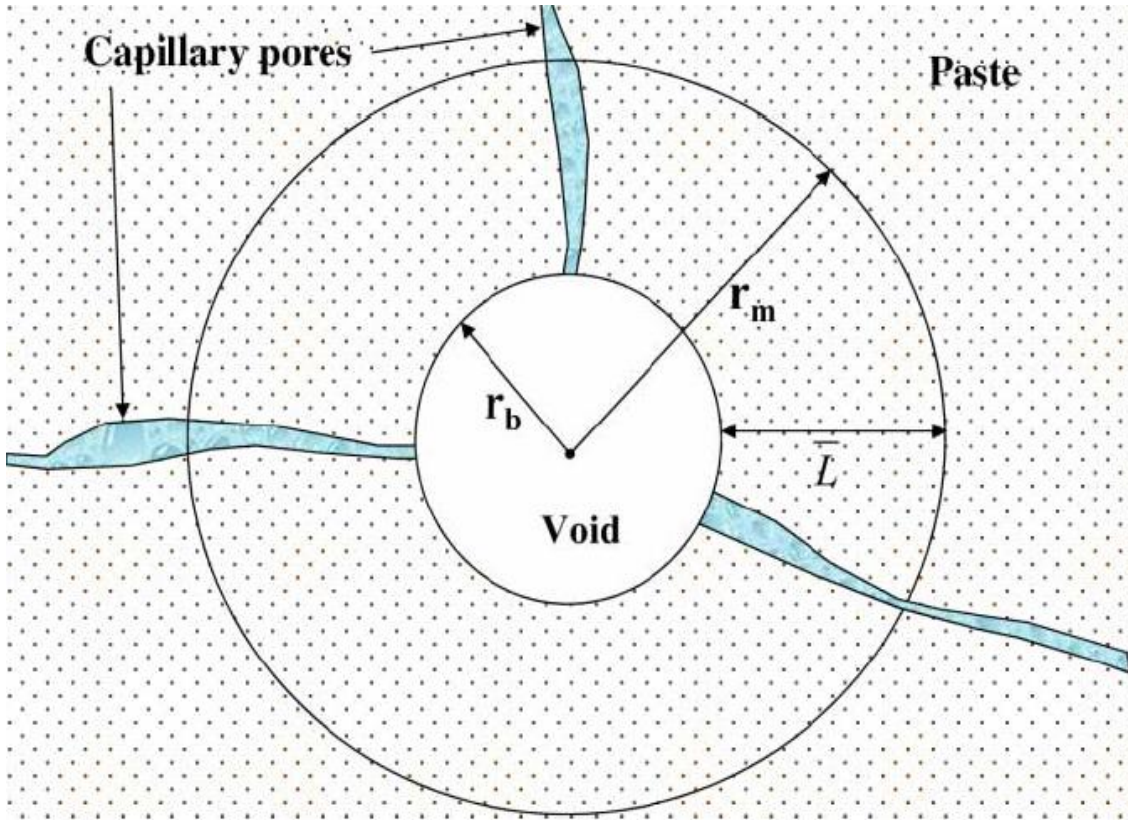


Figure 1. Power's model for a paste shell surrounding an air void

Powers provided the hydraulic theory as follows:

$$\text{Equation 1} \quad p(r = r_m) = \frac{\eta}{K} \left(1.09 - \frac{1}{S_f} \right) \frac{dw_f}{dt} \frac{1}{3} \left(\frac{\bar{L}^3}{r_b} + \frac{3}{2} \bar{L}^2 \right),$$

Where K = the permeability in the cement paste (m^2),

η = viscosity of water (Ns/m^2),

S_f = effective degree of saturation of cement paste outside the air void. (It can be defined as $S_f = \frac{V_f}{V_f+a}$, in which V_f is the volume of freezable water and a is the volume of air contained in the pore system [8].),

$\frac{dw_f}{dt}$ = the percentage of freezable water per second (cm^3/cm^3*s).

Here listed is the selection of default values of parameters for the present study in Table 1.

Table 1. Default Values Selection

Parameter	Selected range (value)
Viscosity η of water at 0°C	1.787Ns/m ² *10 ⁻³
Coefficient of permeability, K	0.40-8.00 m/s *10 ⁻¹³ (1.60m/s *10 ⁻¹³ selected)
Degree of saturation, S_f	80% to 100% (92% selected)
Rate of ice formation, dw_f/dt	0.0-1.0m ³ /m ³ *s(0.25 selected)
Spacing factor, \bar{L}	1.3-2.3*10 ⁻⁴ m (2.1*10 ⁻⁴ m selected)
Radius for entrained air void, r_b	100 μm
Maximum tensile strength, P	650psi

Equation 1 illustrates how different factors affect hydraulic pressure. To assess the maximum spacing factor \bar{L} , calculations has been completed as shown in Tables 2-5. Each of the parameters are chosen based on the theoretic value and calculation. Figures 2, 4, 6, and 8 are drawn according to these four tables.

Table 2, and Figures 2 and 3 show the relationships between the maximum pore pressures with an effective degree of saturation by fixing other parameters. It is reasonable that no damage will occur if the cement paste is below a certain degree of saturation, since the amount of ice formation is not sufficient to fill the voids and cause damage. Experimental results show only the effective degree of saturation above 90%, will occur significant frost damage [9]. From Figure the critical effective degree of saturation is about 92% for the range of parameters selected. This is close to the 90% value reported in the literature.

Table 3, and Figures 4 and 5 show the effect of rate of ice formation on pore pressure. If the rate of ice formation is slower, it provides greater chance for hydraulic pressure to dissipate in capillaries [10]. According to Cai [11], the freezing rate of pore solution is quicker in the range of 0°C ~ -10°C than below -10°C. Since a higher rate of ice formation contributes to higher pore water pressure, the cement paste endures more pressure from freezing, once the temperature is between 0 and -10°C. Below -10°C, the rate of ice formation is low, which means that frost damage can be neglected [11]. From Figure 5, pore pressure will increase with increasing rate of ice formation.

As shown in Table 4, and Figures 6 and 7, permeability is related to pore pressure. There are some indirect relationships between cement paste's permeability and maximum spacing factor. In general, higher permeability will lead to a better connection between the air void systems. In this way, freezing water will move more readily to the nearest escape boundary and release the hydraulic pressure. However, more air voids will reduce the strength of cement paste. In other words, there is a balance point. In Figure the maximum pore pressure drops significantly with increasing permeability up to 2×10^{-11} cm/s. Beyond this value, increasing

permeability has little influence on maximum pore pressure. However, in this region, the impact of permeability on cement paste's tensile strength is significant.

Table 4 and Figure 8 illustrate the relationship between the spacing factor and maximum pore pressure. As expected pore pressure increases with increasing spacing factor. Based on these results, the maximum spacing factor can be assessed. Assuming a tensile strength of about 650 psi [8] and a water permeability of around $1.0-2.0 \times 10^{-11}$ cm/s [12] the maximum spacing factor should be around 2.1×10^{-4} m. These results are consistent with the literature.

Figures 9, 10, and 11 have been drawn to directly determine how permeability, rate of ice formation, and the effective degree of saturation contribute to the spacing factor at the same time. Decreasing both rate of ice formation and effective degree of saturation lead to longer, safe travel distance for water in cement paste. Moreover, increasing permeability also contributes to a larger spacing factor. By comparing these three graphs, the impact of rate of ice formation on the spacing factor is the smallest, when comparing with permeability and effective degree of saturation.

Table 2. Maximum pore pressure vs. effective degree of saturation of the cement paste outside of the air void

η , Viscosity of Water (Ns/m ² *10 ⁻³) at 0°C	K, Permeability of the Cement Paste (m ² *10 ⁻²⁰)	Sf, Effective Degree of Saturation of the Cement Paste Outside the Air Void	dwf/dt, Rate of Ice Formation, (m ³ /m ³ *s)	L, Distance the Water Travels in Capillary Pores (um)	rb, Diameter of Void (m*10 ⁻⁴)	P (r=rm), Maximum Pore Pressure (N/m ²)	P (r=rm), Maximum Pore Pressure (psi)
1.787	1.6	0.8	0.25	210	1	236420100	-34290
1.787	1.6	0.81	0.25	210	1	213617235	-30983
1.787	1.6	0.82	0.25	210	1	191370538	-27756
1.787	1.6	0.83	0.25	210	1	169659906	-24607
1.787	1.6	0.84	0.25	210	1	148466194	-21533
1.787	1.6	0.85	0.25	210	1	127771157	-18532
1.787	1.6	0.86	0.25	210	1	107557400	-15600
1.787	1.6	0.87	0.25	210	1	-87808327	-12736
1.787	1.6	0.88	0.25	210	1	-68508097	-9936
1.787	1.6	0.89	0.25	210	1	-49641580	-7200
1.787	1.6	0.9	0.25	210	1	-31194319	-4524
1.787	1.6	0.91	0.25	210	1	-13152492	-1908
1.787	1.6	0.92	0.25	210	1	4497121	650
1.787	1.6	0.93	0.25	210	1	21767173	315
1.787	1.6	0.94	0.25	210	1	38669777	5609
1.787	1.6	0.95	0.25	210	1	55216537	8009
1.787	1.6	0.96	0.25	210	1	71418572	10358
1.787	1.6	0.97	0.25	210	1	87286545	12660
1.787	1.6	0.98	0.25	210	1	102830681	14914
1.787	1.6	0.99	0.25	210	1	118060795	17123
1.787	1.6	1	0.25	210	1	132986306	19288

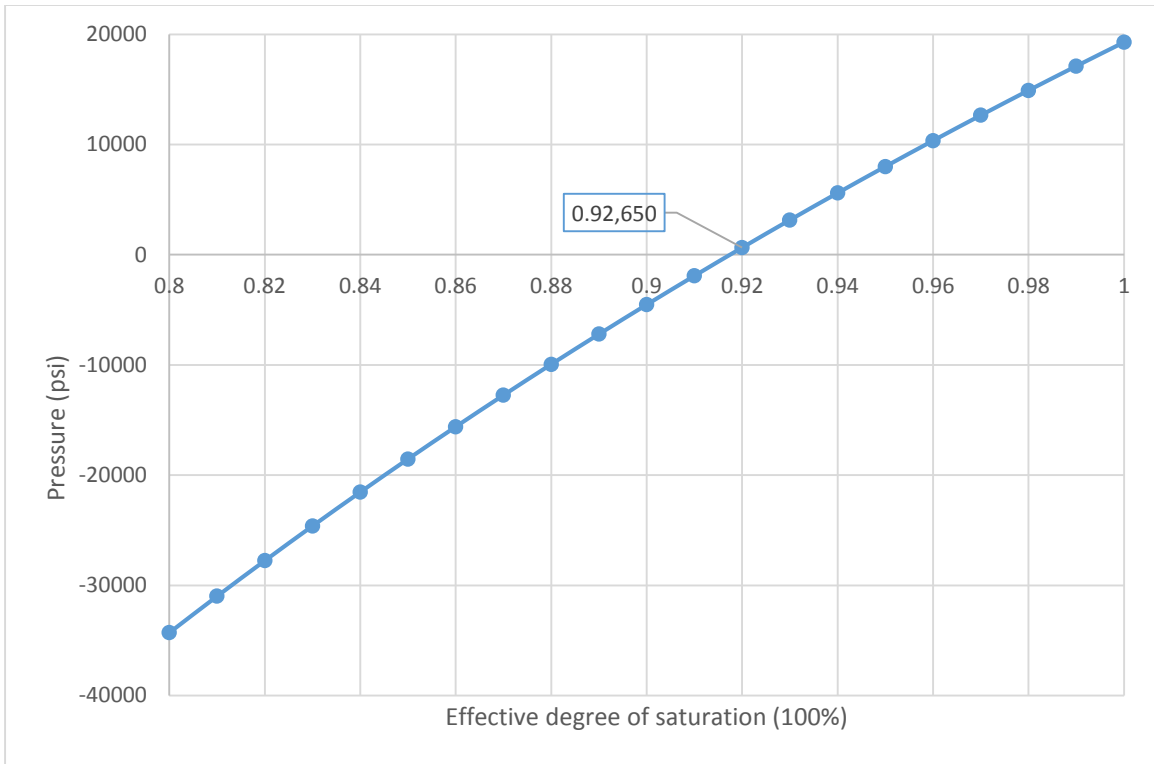


Figure 2. Effect of degree of saturation on maximum pore pressure

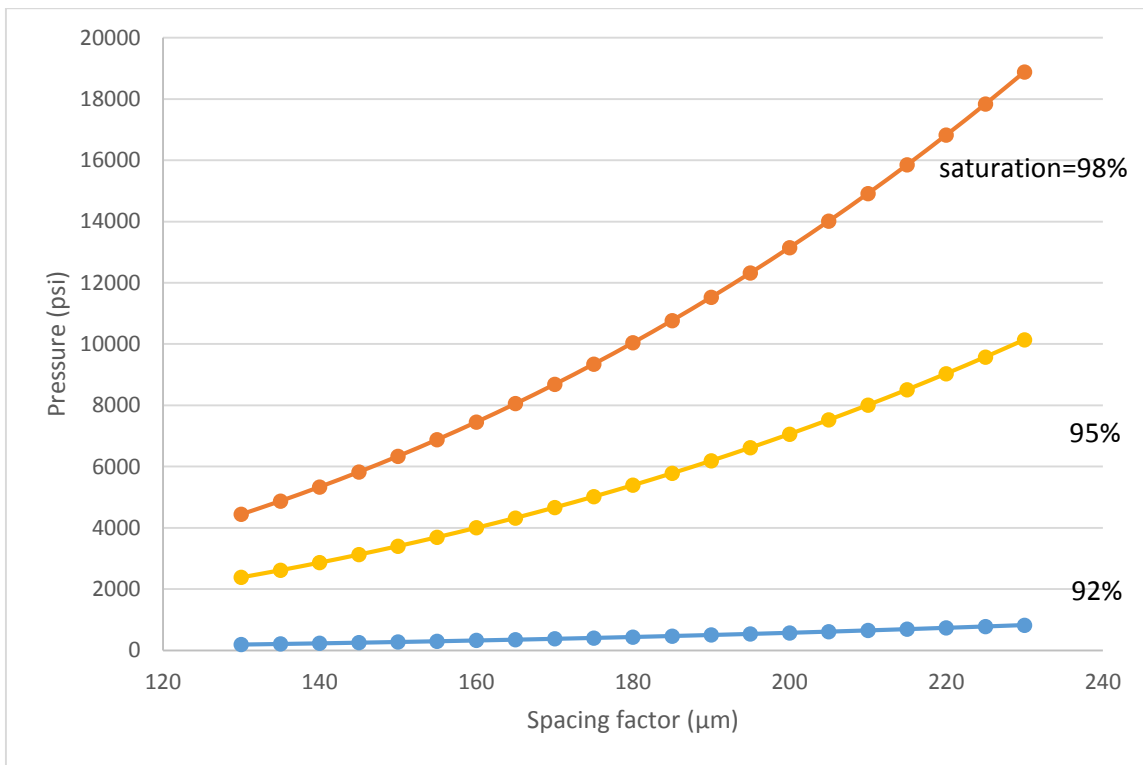


Figure 3. Effect of saturation and spacing factors on maximum pore pressure

Table 3. Maximum pore pressure vs. rate of ice formation

η , Viscosity of Water (Ns/m ² *10 ⁻³) at 0°C	K, Permeability of the Cement Paste (m ² *10 ⁻²⁰)	Sf, Effective Degree of Saturation of the Cement Paste Outside the Air Void	dwf/dt, Rate of Ice Formation, (m ³ /m ³ *s)	L, Distance the Water Travels in Capillary Pores (um)	rb, Diameter of Void (m*10 ⁻⁴)	P (r=rm), Maximum Pore Pressure (N/m ²)	P (r=rm), Maximum Pore Pressure (psi)
1.787	1.6	0.92	0	210	1	0	0
1.787	1.6	0.92	0.05	210	1	899424	130
1.787	1.6	0.92	0.1	210	1	1798849	261
1.787	1.6	0.92	0.15	210	1	2698273	391
1.787	1.6	0.92	0.2	210	1	3597697	522
1.787	1.6	0.92	0.25	210	1	4497121	650
1.787	1.6	0.92	0.3	210	1	5396546	783
1.787	1.6	0.92	0.35	210	1	6295970	913
1.787	1.6	0.92	0.4	210	1	7195394	1044
1.787	1.6	0.92	0.45	210	1	8094819	1174
1.787	1.6	0.92	0.5	210	1	8994243	1305
1.787	1.6	0.92	0.55	210	1	9893667	1435
1.787	1.6	0.92	0.6	210	1	10793092	1565
1.787	1.6	0.92	0.65	210	1	11692516	1696
1.787	1.6	0.92	0.7	210	1	12591940	1826
1.787	1.6	0.92	0.75	210	1	13491364	1957
1.787	1.6	0.92	0.8	210	1	14390789	2087
1.787	1.6	0.92	0.85	210	1	15290213	2218
1.787	1.6	0.92	0.9	210	1	16189637	2348
1.787	1.6	0.92	0.95	210	1	17089062	2479
1.787	1.6	0.92	1	210	1	17988486	2609

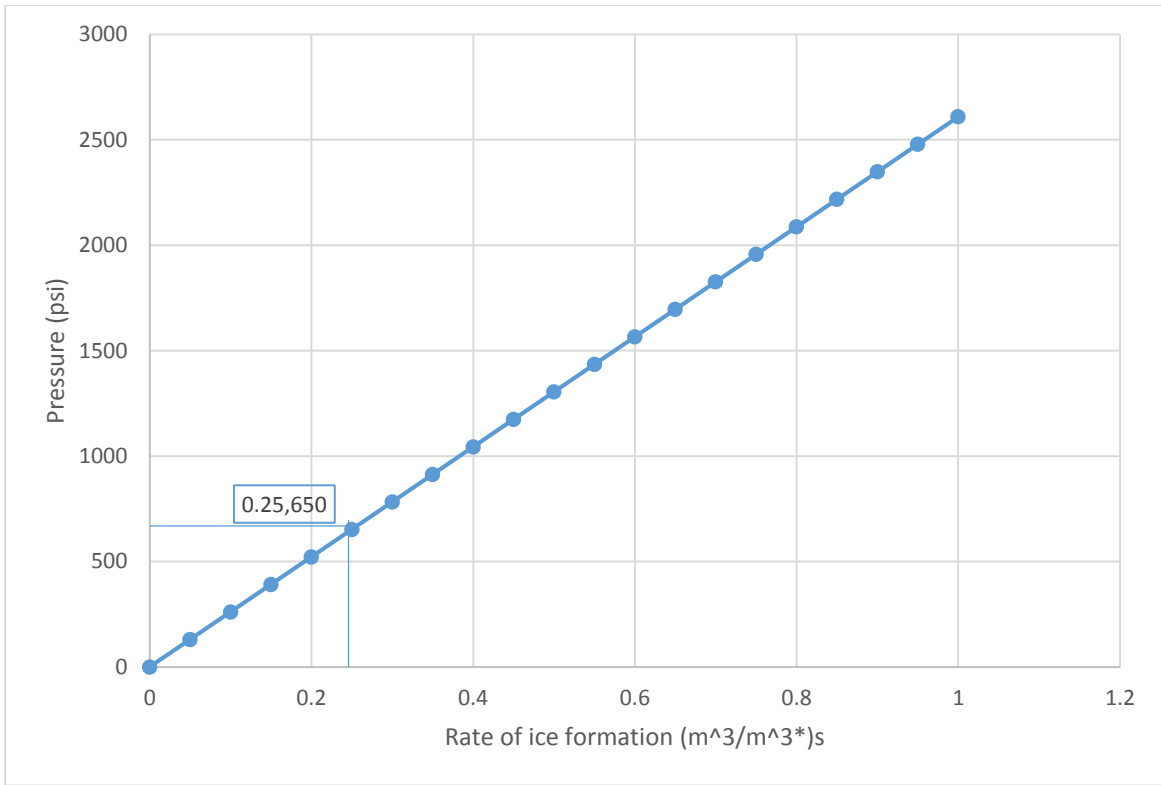


Figure 4. Effect of rate of ice formation on maximum pore pressure

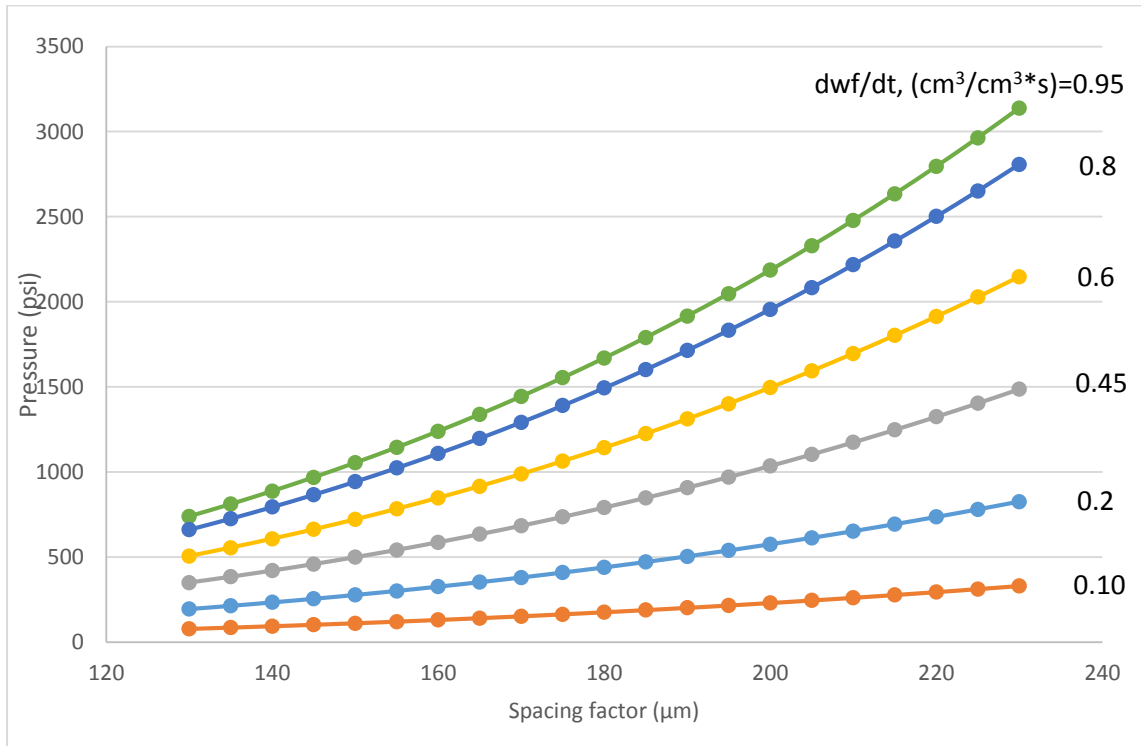


Figure 5. Effect of rate of ice formation and spacing factor on maximum pore pressure

Table 4. Maximum pore pressure vs. permeability

η , Viscosity of Water (Ns/m ² * 10 ⁻³) at 0°C	K, Permeability of the Cement Paste (m ² *10 ⁻²⁰ =m/s*10 ¹³)	Sf, Effective Degree of Saturation of the Cement Paste Outside the Air Void	dwf/dt, Rate of Ice Formation, (m ³ /m ³ *s)	L, Distance the Water Travels in Capillary Pores (um)	rb, Diameter of Void (m*10 ⁻⁴)	P (r=rm), Maximum Pore Pressure (N/m ²)	P (r=rm), Maximum Pore Pressure (psi)
1.787	0.4	0.92	0.25	210	1	17988486	2609
1.787	0.8	0.92	0.25	210	1	8994243	1305
1.787	1.2	0.92	0.25	210	1	5996162	870
1.787	1.6	0.92	0.25	210	1	4497121	650
1.787	2	0.92	0.25	210	1	3597697	522
1.787	2.06	0.92	0.25	210	1	3492910	507
1.787	2.4	0.92	0.25	210	1	2998081	435
1.787	2.8	0.92	0.25	210	1	2569784	373
1.787	3.2	0.92	0.25	210	1	2248561	326
1.787	3.6	0.92	0.25	210	1	1998721	290
1.787	4	0.92	0.25	210	1	1798849	261
1.787	4.4	0.92	0.25	210	1	1635317	237
1.787	4.8	0.92	0.25	210	1	1499040	217
1.787	5.2	0.92	0.25	210	1	1383730	201
1.787	5.6	0.92	0.25	210	1	1284892	186
1.787	6	0.92	0.25	210	1	1199232	174
1.787	6.4	0.92	0.25	210	1	1124280	163
1.787	6.8	0.92	0.25	210	1	1058146	153
1.787	7.2	0.92	0.25	210	1	999360	145
1.787	7.6	0.92	0.25	210	1	946762	137
1.787	8	0.92	0.25	210	1	899424	130

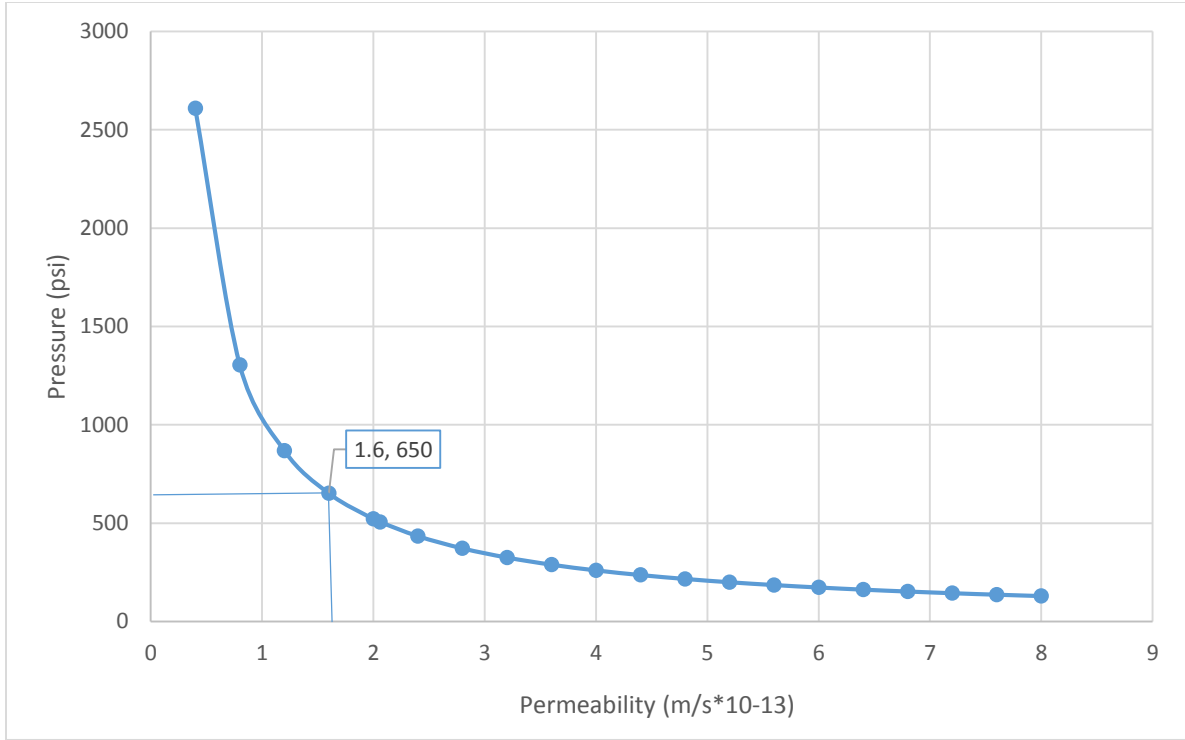


Figure 6. Effect of rate of permeability on maximum pore pressure

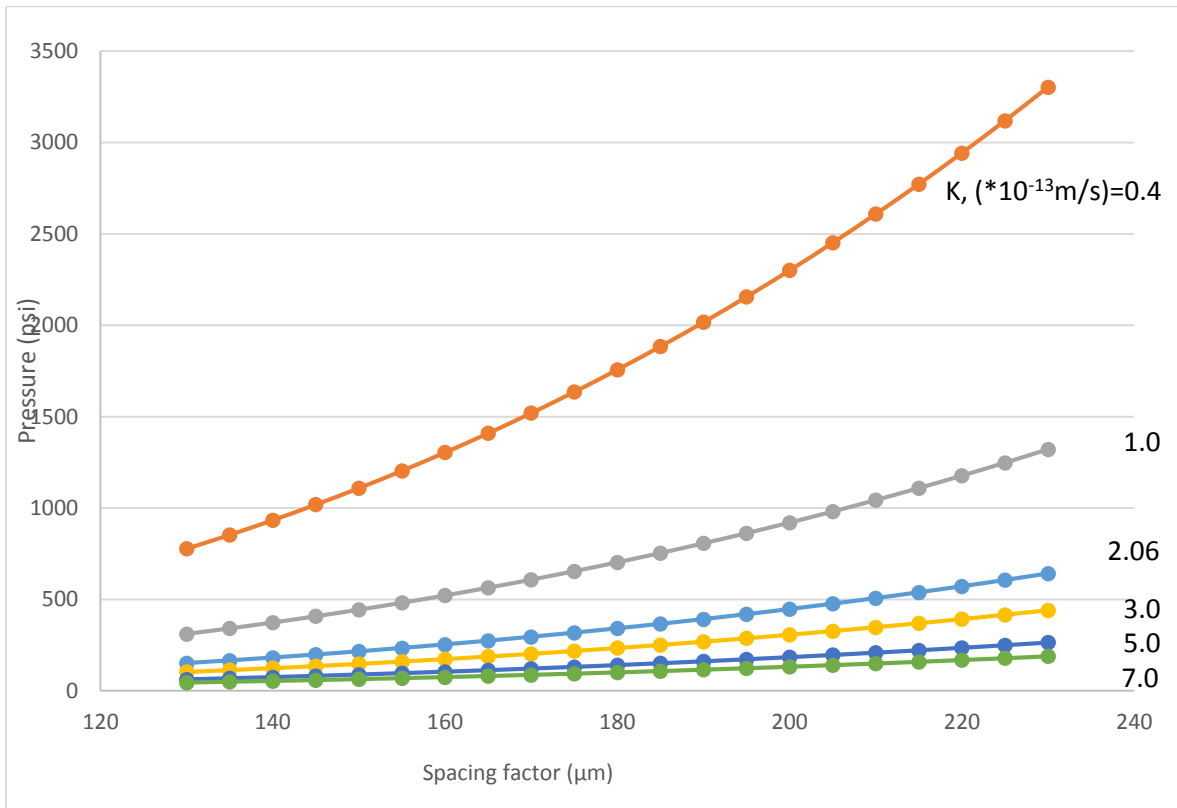


Figure 7. Effect of permeability and spacing factor on maximum pore pressure

Table 5. Maximum pore pressure vs. distance water travels in capillary pores

η , Viscosity of Water (Ns/m ² *10 ⁻³) at 0°C	K, Permeability of the Cement Paste (m ² *10 ⁻²⁰)	Sf, Effective Degree of Saturation of the Cement Paste Outside the Air Void	dwf/dt, Rate of Ice Formation, (m ³ /m ³ *s)	L, Distance the Water Travels in Capillary Pores (um)	rb, Diameter of Void (m*10 ⁻⁴)	P (r=rm), Maximum Pore Pressure (N/m ²)	P (r=rm), Maximum Pore Pressure (psi)
1.787	1.6	0.92	0.25	130	1	1340412	194
1.787	1.6	0.92	0.25	135	1	1471316	213
1.787	1.6	0.92	0.25	140	1	1610081	234
1.787	1.6	0.92	0.25	145	1	1756918	255
1.787	1.6	0.92	0.25	150	1	1912041	277
1.787	1.6	0.92	0.25	155	1	2075663	301
1.787	1.6	0.92	0.25	160	1	2247994	326
1.787	1.6	0.92	0.25	165	1	2429249	352
1.787	1.6	0.92	0.25	170	1	2619638	380
1.787	1.6	0.92	0.25	175	1	2819376	409
1.787	1.6	0.92	0.25	180	1	3028674	439
1.787	1.6	0.92	0.25	185	1	3247744	471
1.787	1.6	0.92	0.25	190	1	3476800	504
1.787	1.6	0.92	0.25	195	1	3716053	539
1.787	1.6	0.92	0.25	200	1	3965716	575
1.787	1.6	0.92	0.25	205	1	4226001	613
1.787	1.6	0.92	0.25	210	1	4497121	650
1.787	1.6	0.92	0.25	215	1	4779289	693
1.787	1.6	0.92	0.25	220	1	5072717	736
1.787	1.6	0.92	0.25	225	1	5377617	780
1.787	1.6	0.92	0.25	230	1	5694201	826

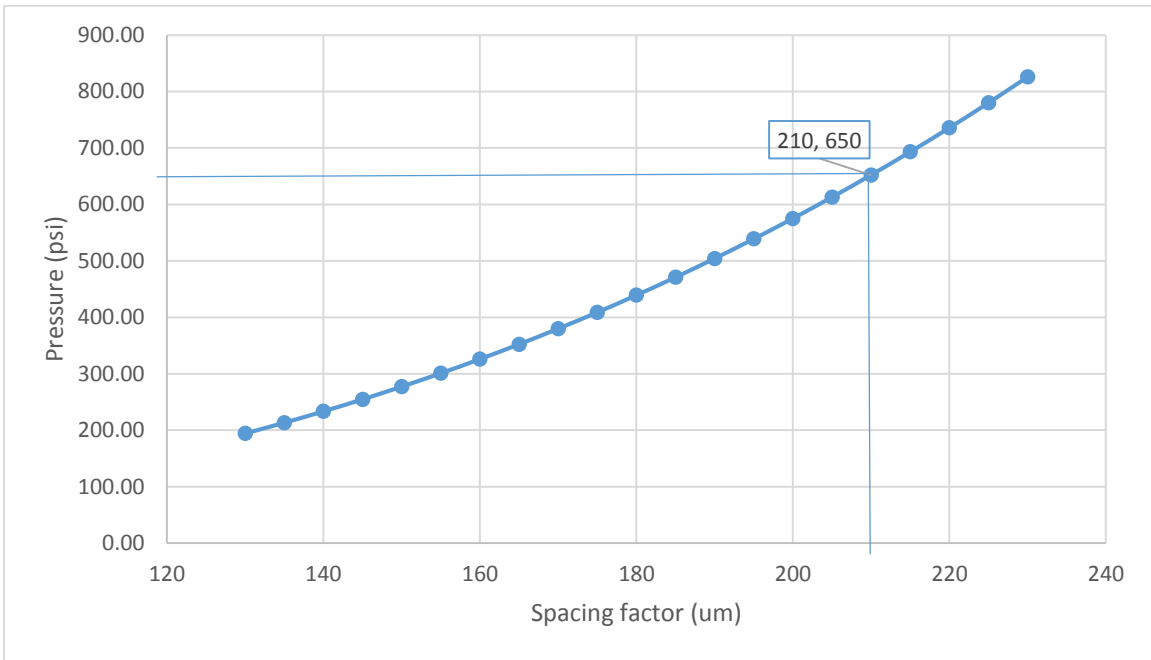


Figure 8. Effect of spacing factor on maximum pore pressure

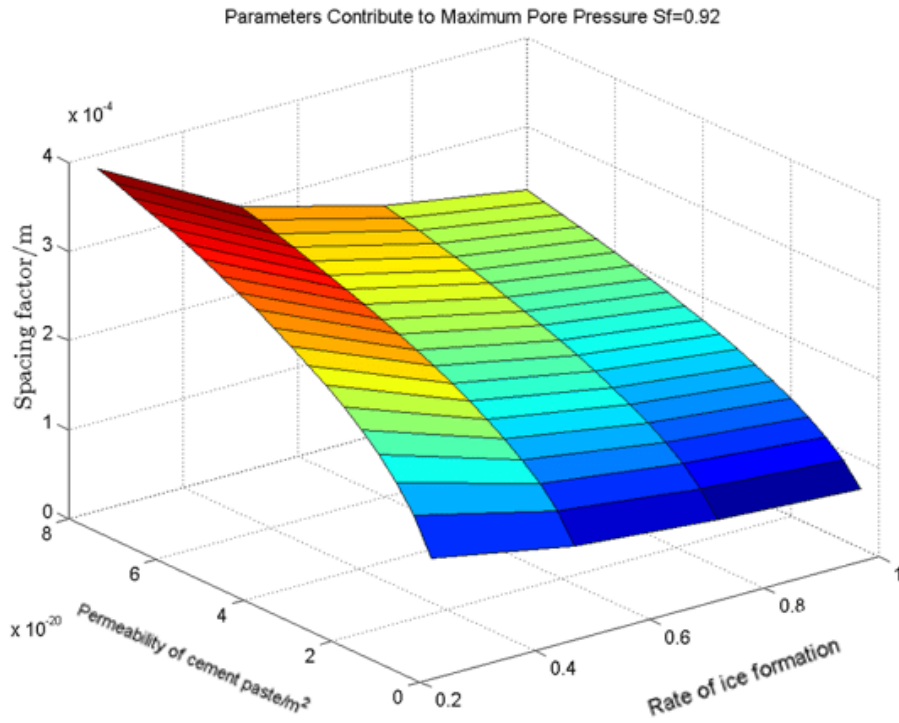


Figure 9. Parameters contribute to maximum pore pressure Sf=0.92

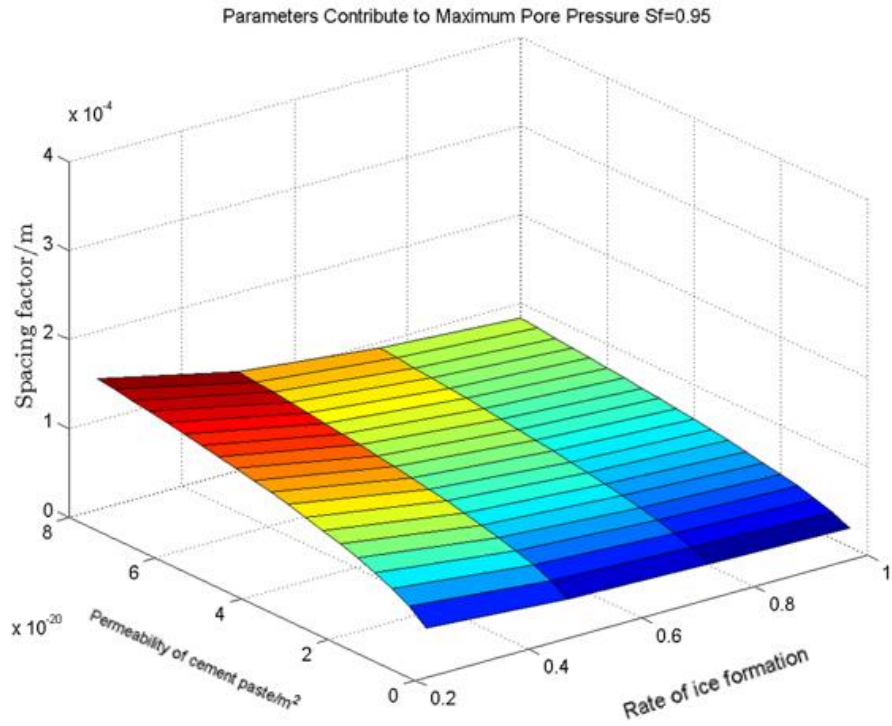


Figure 10. Parameters contribute to maximum pore pressure Sf=0.95

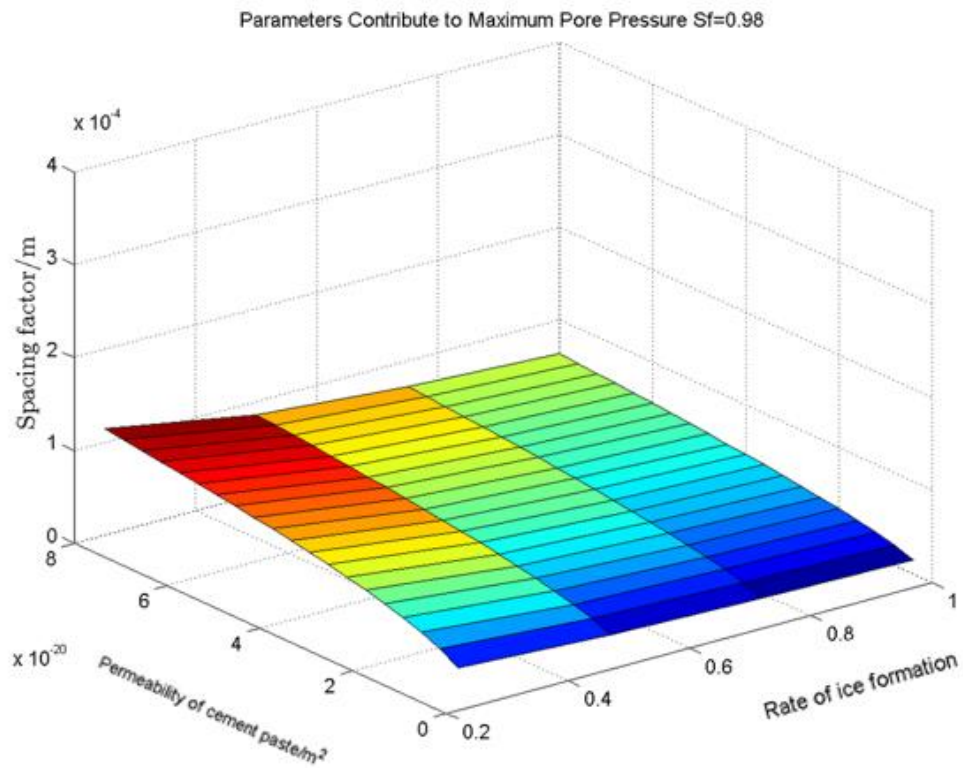


Figure 11. Parameters contribute to maximum pore pressure Sf=0.98

3.3 Conclusions

The following conclusions can be drawn from the present study:

- The maximum spacing factor should be around 210 μ m for maximum pore pressure of 650psi (consistent with the values proposed by Powers in 1949). The pore pressure increases with increased spacing factor.
- For given $\eta=1.787$ Ns/m², $r_b=100\mu$ m, $K=1.6*10^{-11}$ cm/s, $dwf/dt=0.25m^3/m^3*s$, $\bar{L}=210\mu$ m, the maximum pore pressure reaches 650psi when effective degree of saturation is 0.92. The pore pressure increases with increased degree of saturation.
- For given $\eta=1.787$ Ns/m², $r_b=100\mu$ m, $K=1.6*10^{-11}$ cm/s, $S_f=0.92$, $\bar{L}=210\mu$ m, the maximum pore pressure reaches 650psi when rate of ice formation is $0.25m^3/m^3*s$. The pore pressure increases with increased rate of ice formation.
- For given $\eta=1.787$ Ns/m², $r_b=100\mu$ m, $S_f=0.92$, $dwf/dt=0.25m^3/m^3*s$, $\bar{L}=210\mu$ m, the maximum pore pressure reaches 650psi when permeability is $1.6*10^{-11}$ cm/s. The pore pressure increases with decreased permeability.
- Spacing factor requirement for F-T resistance ($P < 650psi$) frost may vary depends upon degree of saturation, rate of ice formation, and permeability.

References

- [1] P. Kumar Mehta, Paulo J.M. Monteiro, *Concrete Microstructure, Properties, and Materials*, Department of Civil and Environmental Engineering: McGraw-Hill, 2006.
- [2] "Penetron, Total Concrete Protection, Internal Waterproofing for Concrete," March 2010. [Online]. Available: <http://www.penetron.com/newsletter/mar10-en.htm>. [Accessed 10 11 2013].
- [3] Y. Ballim, "A low cost, falling head permeameter for measuring concrete gas permeability," *Concrete Beton*, p. 13, November 1991.
- [4] A. M. Neville, *Properties of concrete*, New York, 1996, p. 844.
- [5] K. Hover, "Why is there air in concrete," *Concrete Construction*, 1993.
- [6] D. Burden, "The durability of concrete containing high levels of fly ash," PCA, Skokie, 2006.
- [7] T. C. Powers, L. E. Copeland, J. C. Hayes, H. M. Mann, "Permeability of Portland Cement Paste," *Journal of the American Concrete Institute*, vol. 51, p. 285, April 1955.
- [8] T. C. Power, "The Physical Structure and Engineering Properties of Concrete," *Portland Cement Association*, vol. Bulletin 90, 1958.
- [9] C. C. Jr., *Microscopic Observations of Internal Frost Damage and Salt Scaling*, University of California, Berkeley: UMI Dissertations Publishing, 2008.
- [10] F. P. Glasser, "Thermodynamics of Cement Hydration," *Materials Science of Concrete VII*, 2005.
- [11] Jussara Tanesi and Richard Meininger, "Freeze-thaw resistance of concrete with marginal air content," December 2006.
- [12] T. C. Powers, R. A. Helmuth, "Theory of Volume Changes in Hardened Portland-Cement Paste During Freezing," *Highway Research Board*, p. 32, 1953.

List of Figures

Figure 1. Power's model for a paste shell surrounding an air void	21
Figure 2. Effect of degree of saturation on maximum pore pressure.....	26
Figure 3. Effect of saturation and spacing factors on maximum pore pressure.....	26
Figure 4. Effect of rate of ice formation on maximum pore pressure.....	28
Figure 5. Effect of rate of ice formation and spacing factor on maximum pore pressure	28
Figure 6. Effect of rate of permeability on maximum pore pressure.....	30
Figure 7. Effect of permeability and spacing factor on maximum pore pressure.....	30
Figure 8. Effect of spacing factor on maximum pore pressure.....	32
Figure 9. Parameters contribute to maximum pore pressure Sf=0.92	32
Figure 10. Parameters contribute to maximum pore pressure Sf=0.95	33
Figure 11. Parameters contribute to maximum pore pressure Sf=0.98	33

List of Tables

Table 1. Default Values Selection	22
Table 2. Maximum pore pressure vs. effective degree of saturation of the cement paste outside of the air void	295
Table 3. Maximum pore pressure vs. rate of ice formation	27
Table 4. Maximum pore pressure vs. permeability.....	29
Table 5. Maximum pore pressure vs. distance water travels in capillary pores	31

CHAPTER IV. FALLING HEAD PERMEAMETER FOR MEASURING CEMENT

PASTE WATER PERMEABILITY

A Paper to be submitted to Transportation Research Board

Xinyao Li⁴, Peter C. Taylor⁵, and Kejin Wang⁶

Abstract

This paper describes the development and evaluation of a falling head permeameter for measuring water permeability of saturated cement paste. The apparatus is developed based on an existing device used to measure gas permeability of concrete. The paper discusses the background to the method and the activities conducted to minimize variability in the test data.

Keywords: Permeameter, water permeability, falling head, cement paste

⁴ Graduate Student, Iowa State University, Civil, Construction and Environmental Engineering, 136 Town Engineering, Ames, IA 50011, Tel: 515-817-3012, Email: xli@iastate.edu

⁵ Director II, National Concrete Pavement Technology Center, Iowa State University, Ames, IA 50011, Tel: 515-294-9333, Email: ptaylor@iastate.edu

⁶ Professor, Iowa State University, Civil, Construction and Environmental Engineering, 492 Town Engineering, Ames, IA 50011, Tel: 515-294-5126, Fax: 515-294-8216, Email: kejinw@iastate.edu

4.1 Introduction

All environmental based deterioration mechanisms in concrete, including freeze thaw distress, involve moisture transport. In order to improve the durability of cement paste under severe conditions, the ability to measure of water transport properties of a mixture is significant. However, there are at present few good tests that have been accepted for water permeability measurement. For this reason, this paper presents the development of a new falling head permeameter to be used for measuring cement paste water permeability.

4.1.1 Permeability of cement paste

Permeability is the property that describes the rate of flow of a fluid through a material under a pressure gradient. Because concrete is comprised of a dense matrix, the permeability is low, making it difficult to measure with precision.

Hardened cement paste is a porous solid and not an aggregation of discrete particles [1]. Hence, Darcy's law has been adopted here to estimate the relationship between rate of flow and hydraulic pressure in hydrated cement paste with different permeabilities.

4.1.1.1 Capillary flow

Darcy's law describes the flow in capillary pores for laminar flow through porous media:

$$\frac{dq}{dt} = KA \left(\frac{\Delta h}{L} \right) = KA^2 \frac{\Delta h}{A L},$$

Where dq/dt = rate of fluid flow (in^3/s or cm^3/s),

K =coefficient of permeability (in/s or cm/s),

ΔH =difference in pressure head (in. or cm),

A= surface area (in² or cm²), and

L= thickness of the concrete (in. or cm).

Note: $\Delta H = \Delta P / \rho$,

Where ΔP = pressure difference (in lbf/in² or kgf/cm²),

ρ = density of fluid (in lbf/in³ or kgf/cm³), and

$$P = \frac{\Delta h}{A}$$

Assume L=1cm and A=10cm²(cross-section area of the specimen). Then the rate of flow can be write as

$$\frac{dq}{dt} = K * 100 * P .$$

According to this equation, the graph below can be drawn as Figure 1.

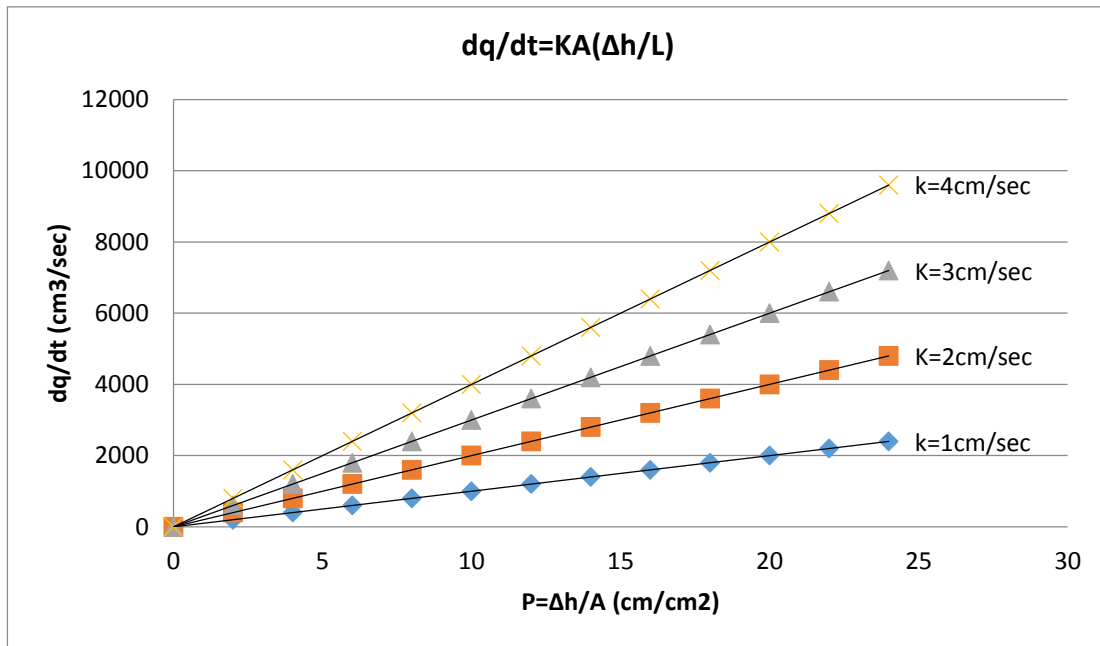


Figure 1. Flow rate vs. pressure for porous media with different permeability

Figure 1 and the appendix illustrate the rate of flow will increase when hydraulic pressure increases for a given permeability of a certain type of cement paste.

There are other factors affecting permeability of cement paste. The degree of hydration and water to cement ratio are the two major factors. In general, when the water to cement ratio is high and the degree of hydration is low, the cement paste will have a higher permeability [2]. The reason is the longer the curing time for cement paste causes the capillary pores to become smaller and become disconnected.

4.1.2 Approach to challenges

Limitations of the existing systems then include:

- Results are extremely sensitive to moisture state of the sample
- Flow through the concrete is non-linear
- Devices are expensive

The approach discussed in this paper was to address some of these concerns, in particular the first, by conducting tests on a pre-saturated sample, which is much easier to achieve than some known or controlled partial moisture state.

The approach taken was is to take the Ballim oxygen test and invert the device with some minor changes. The same sample can be tested at different ages to evaluate the relationship between degree of hydration and water permeability. There are several advantages for this test comparing with the others. The major advantage is the cost is much lower. Besides, the operation is really simple. As for the testing period, the data recording period is less than 24 hours which is relatively short.

4.2 Materials and Mix Proportion

Experiments were designed to characterize water permeability of cement paste. Type I/II Portland cement was used. A Type 1 water reducer (WRA) was used as needed to modify the workability and flowability of the fresh cement paste.

Mixing was conducted in a high shear mixer, then samples were kept in a horizontal rotator until set to reduce the effects of bleeding. Figures 2 and 3 show these two devices. The reason for using a high shear mixer is to prevent segregation. The speed of the rotator was around 50 rotations/min.

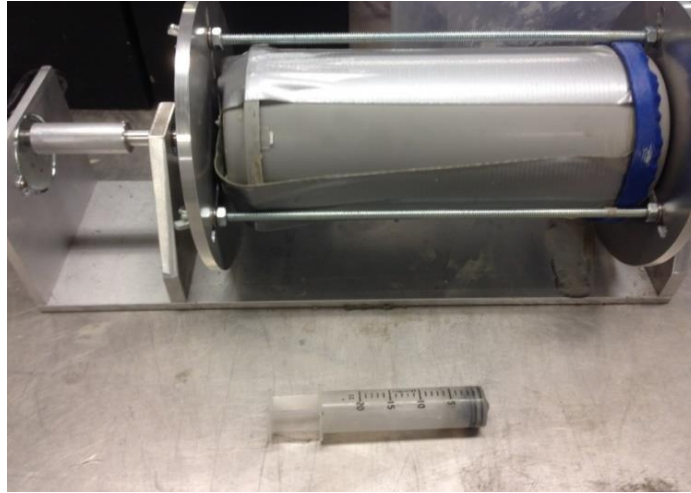


Figure 2. Horizontal rotator



Figure 3. High shear mixer

Table 1 shows the three cement paste mix proportions. For the cement paste mix with $w/c=0.35$ and 0.45 , the dosage of normal range water reducer is 0.8% and 0.4% liquid by weight of cement, respectively.

Table 1. Mix proportions

Group	w/c	Cement (g)	Water (g)	WRA (g)	Total (g)
1. Type I/II cement	0.35	3037	1063	24	4124
2. Type I/II cement	0.45	3000	1350	12	4362
3. Type I/II cement	0.55	3000	1650	0	4650

4.3 Testing Procedures

The following produces are used in the present study:

1. Preparing the specimen: After the scheduled curing age, cut a 1" thick disk from the 4" diameter cylinder and grind off any sharp edges. Mark the specimens and place them in the moisture room between 28 and 35 days.
2. Conditioning the specimen: In a sealable container, boil a liter or more of tap water. Remove it from heat and seal the container, allowing it to cool to ambient temperature. Place both specimen and cooled water in vacuum desiccator. The specimen must be totally immersed in water. Then, tightly cap the desiccator and begin vacuum pump. Within a few minutes, pressure will drop to less than 50mm Hg (6650pa). Ensure the desiccator to be vacuum for 3 h. Then, soak specimen under water in desiccator for 18 ± 2 h [3].
3. Measure the thickness of specimen to the nearest 0.02 mm at four equally spaced points and determine the average dimensions.

4. Installing the specimen in the permeameter: With the compressible collar centered in the 6" diameter ×3" tall stainless steel ring, apply a thin coat of Petroleum Jelly to the bottom surface and inside diameter of the compression collar. Next, insert the specimen into the compressible collar down to 1/2" metal spacer above the specimen. The top edge of the top 1/2" metal spacer should be flush with the compressible collar and the bottom edge of the top 1/2" metal spacer should be in contact with the top of the specimen. After placement, turn the compressible collar upside down.
5. Place the compressible collar assembly on the bottom of the water tank, in the centering groove. Insert the PVC (poly vinyl chloride) ring spacer on the bottom of the compressible collar and then place the metal cover plate over the tie-down bolts. Tighten all bolts evenly, with a medium torque until about 1/4" to 1/8" of wood spacer is visible uniformly upon the metal cover plate.
6. With both air valves closed except for the top air valve, add room temperature tap water through the funnel from the top air valve. When the water level goes up in the water tank and in the middle of the upper pipe, tilt the permeameter in all four directions to allow the air trapped below the top of the water tank to escape. Open the first air valve of the water tank. If water continues to flow from this valve, it means sufficient water has been added at this point of time. Then, allow the excess to water run out of this air valve before closing it. Continuously add 16 ml water until there are 10 ml left for air. Close all air valves and connect the air line to the front/lower inlet valve. Open the valve gently to allow air pressure to build to 30 psi.

7. Begin and record start time for the test, i.e., time=0 and pressure=30psi. Gently tap the pressure gate before taking each reading.
8. Test time depends on permeability and specimen thickness.
9. A visual observation of air bubbles/permeability may be obtained by brushing/wiping a few drops of soapy water on the top surface of the specimen after starting the test.
10. At completion of the test, release all air pressure and leave valves open. Then, drain the water from the tank. Remove the cover plate, PVC spacer, spacer ring, and specimen. Store the top spacer ring, wood spacer, and cover plate on top of the unit with all nuts loosely threaded onto the tie-down bolts, using the ratchet wrench stored on one of the tie-down bolts. Clean the work area.

4.4 Results and Discussion

4.4.1 Sources of error

This test is extremely sensitive to several factors including leakage, temperature variations, volume of initial air, and dissolution of air in water. Effects of each factor have been discussed below.

4.4.1.1 Leakage

To check the air tightness, the apparatus is placed in a large barrel and submerged in water as seen in Figure 4. The method to detect leakage is by adding some soapy water into the water barrel to see if air bubbles emerge. After the modification, there is no bubble observed, which indicates the apparatus is well sealed. Care has to be taken to seal all connections and to ensure that the sample is tightly installed in the apparatus.



Figure 4. Permeameter submerged in water

4.4.1.2 Temperature

Figure 5 illustrates that changes in temperature will influence pressure change observations. Initial tests were conducted in a room with limited heating and cooling controls. Changes in temperature between day and night (50 to 70 °F) are reflected in changes in pressure (28.85 to 29.15psi) in the chamber in a test conducted on an impermeable steel blank. Subsequent tests were conducted in a chamber with a tighter control of temperature.

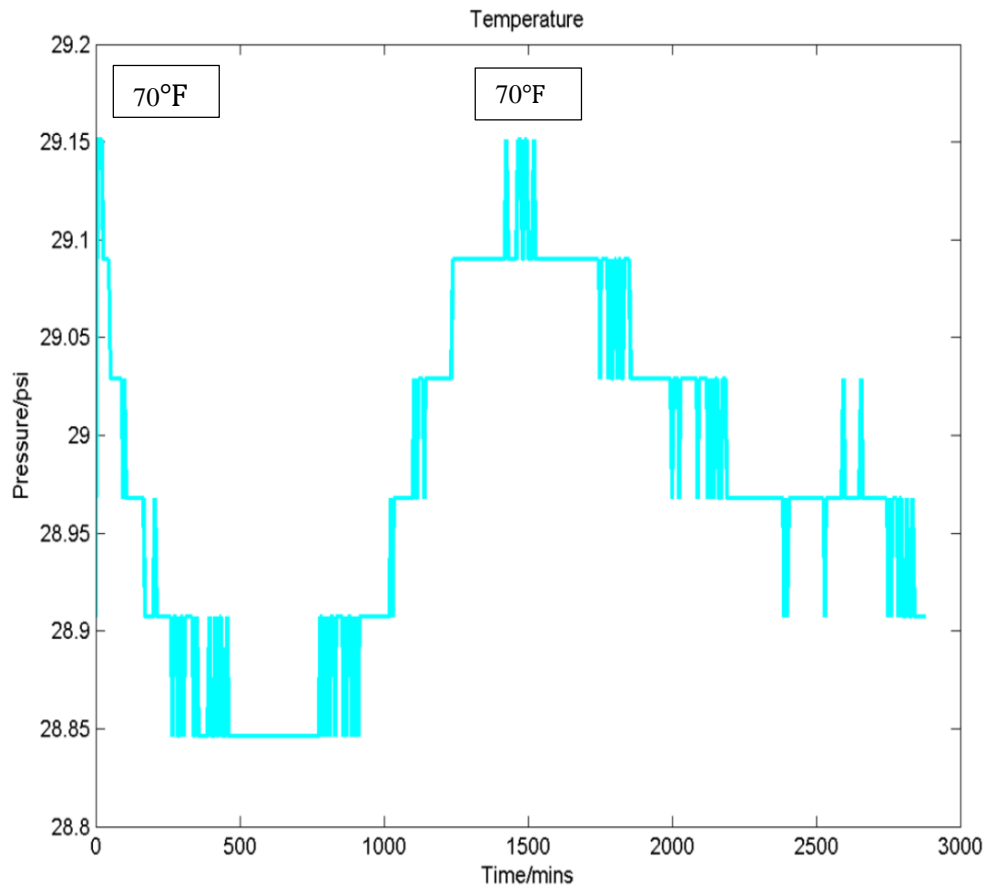


Figure 5. Effect of temperature on permeability measurement (steel plate)

4.4.1.3 Initial air volume

Initial air volume also influences the test results. As indicated above, the initial air volume was selected as 10 mL in order to be sufficiently sensitive to provide measurable data for typical concrete permeability values. However, controlling this volume is delicate, and as shown in Figure 6, for the plastic plate at 70F, a lower initial volume of air results a greater pressure drop, as expected.

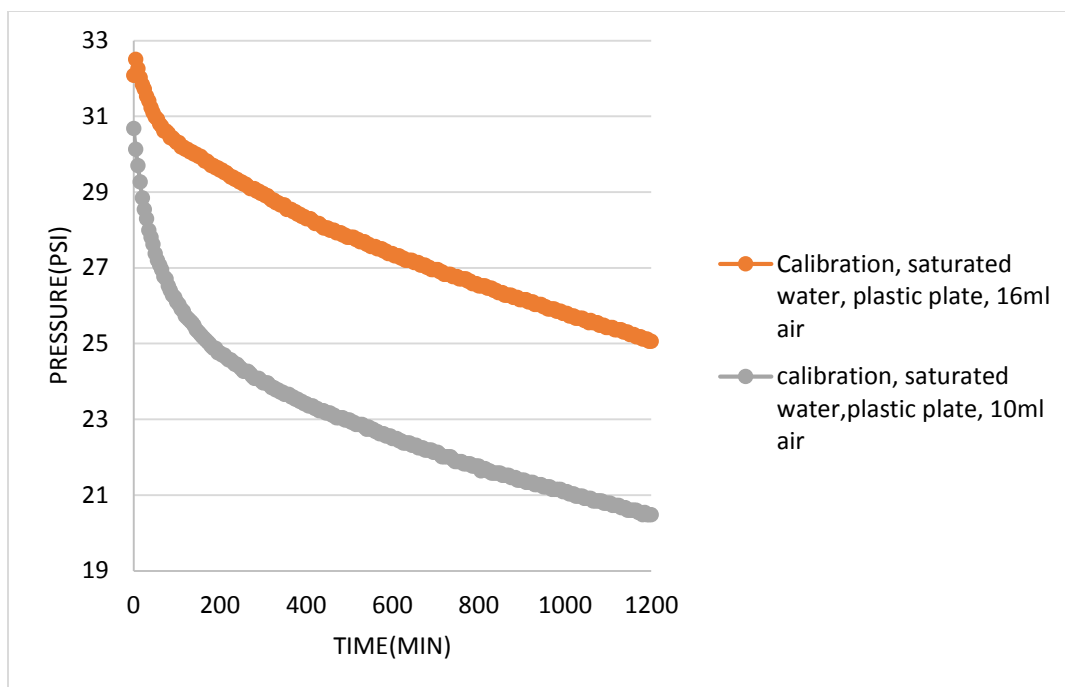


Figure 6. Effect of initial air volume on permeability measurement (at 70°F, steel plate)

4.4.1.4 Degree of air saturation in water

A notable trend was that tests conducted on nominally impermeable blanks, such as steel and plastic, there was still a pressure loss over time. It is believed that this is due to air becoming dissolved into the water. This was investigated by varying the saturation of air in the water used to fill the chamber by means of bubbling air through the water for 24 hours before a test was started.

As seen in Figure 7, if water is saturated with air, the pressure drop is larger. This is abnormal, since air saturated water leaves less opportunity for air dissolving in water, which makes pressure decreasing less significant. From this adverse trend, it indicates the degree of air saturation in water is not the one of major factors affecting test results.

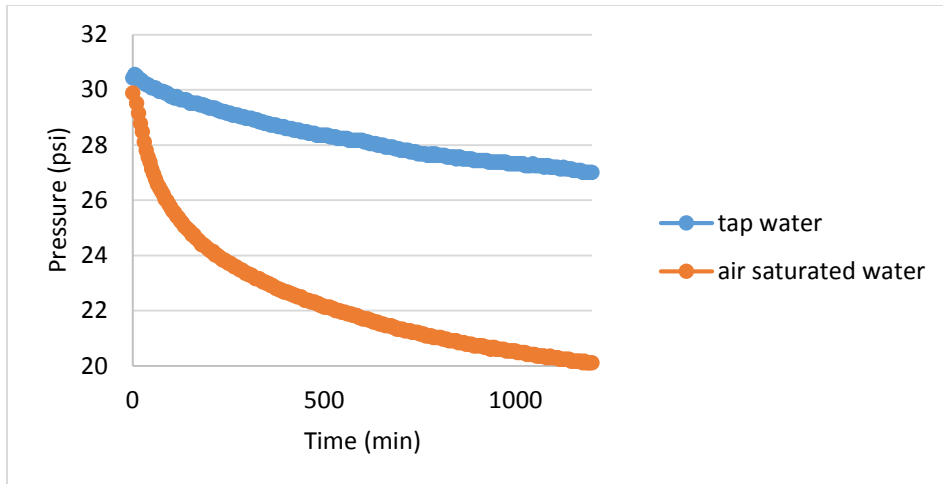


Figure 7. Effect of air saturation on permeability measurement (steel plate)

4.4.1.5 Repeatability

As seen in Figure 8 and Figure 9, tests are completed at 70°F with different specimens. Figure 8 shows the two calibration tests with both steel and plastic plates, the pressure drop is almost the same for each, which illustrates the results for the calibrations are reliable. However, as in Figure 9, when it comes to cement paste specimens, the results are less convincing, and variability between tests of cement paste samples is high.

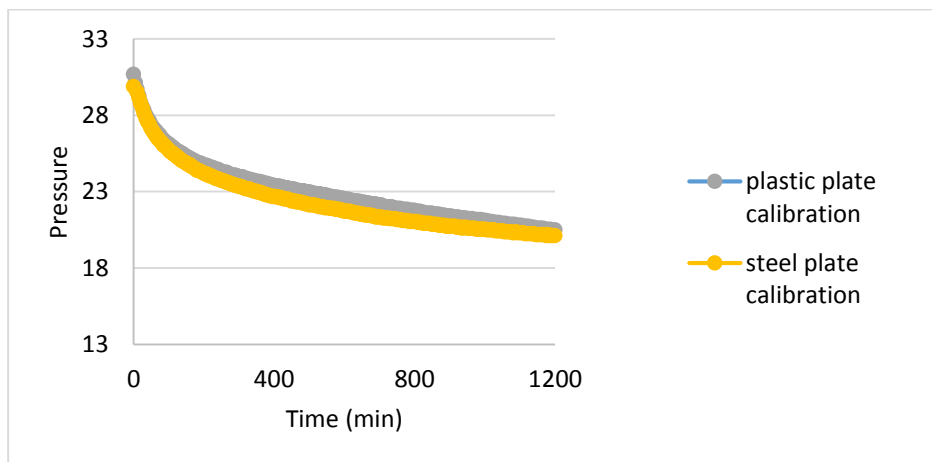


Figure 8. Effect of repeatability on permeability measurement with air saturated water at 70°F (steel plate)

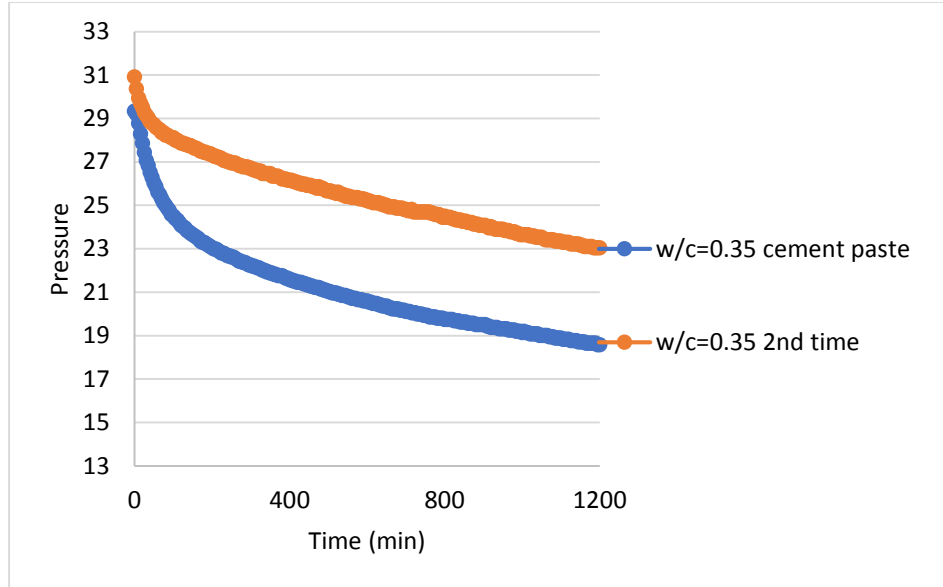


Figure 9. Effect of repeatability on permeability measurement for cement paste of water-to-cement ratio=0.35 with air saturated water at 70°F

4.4.2 Water permeability calculation

Table 2 shows the sample calculation of water permeability.

Table 2. Parameters for Water Permeability Calculation

K, Permeability (cm/s)	A Specimen's area (cm ²)	L Thickness of specimen (cm)	T Time for measurement (s)	h, Applied water head pressure (cm)	$\frac{Q}{t}$ Rate of flow (cm ³ /s)	Q Flow (cm ³)
w/c=0.7, 24 days of hydration, cement paste	2 inches for radius	1 inch for height	20hr	When the initial air pressure equals 30psi=207Kpa		
$1 \cdot 10^{-10}$	81	2.54	1200	$h = (P_1 + P_2) / \rho g$	$\frac{V_2 - V_1}{t}$	$V_2 - V_1$

Boyle's Law:

$$P_1V_1=P_2V_2$$

Initial: leave $V_1=10\text{ cm}^3$ for air. Next, fill the remainder of the tank with water. $P_1=30\text{psi}$;

Measured: $P_2=28.6\text{-}22\text{psi}$.

Then, calculate V_2 . Expected volume, Q , of water (24-48 hours) is

$$Q = V_2 - V_1 ; (Q=0.5\text{-}3.6\text{cm}^3).$$

Assume the system is in the steady flow state,

$Q = KA \frac{h}{L}$ (Darcy's Law), $P = \rho gh$ ($\rho = 1000\text{kg/m}^3$, $g=10\text{m/s}^2$), and $h = P/\rho g$. Then,

$$h = (P_1 + P_2)/\rho g .$$

Hence water permeability can be calculated as, $K = \frac{QL}{A(P_1+P_2)/\rho g}$

As seen in Figure 10, it is drawn by selecting the test results for cement paste samples. Only the lines beneath lines of calibration is reasonable, so these three lines are picked. By subtracting the pressures measured for specimen from steel plate, it is the absolute pressure drop. Figure 11, 12, 13 are absolute pressure drops at 70°F with air saturated water for water-to-cement ratio=0.35, 0.45 and 0.55. By fitting the exponential 3P prediction model, the pressures growth rate can reach zero over time, which means the absolute pressure drop will be constant once the pressure in water tank equals one atmosphere. However, for cement paste with water-to-cement ratio=0.35 and 0.45, the exponential 5P prediction model fits the curve better. If adopting this fit model, the absolute pressure drop will be continuously increasing, which is unreasonable. For this reason, exponential 3P model has been used to predict the trend in this study. By subtracting this constant absolute value of pressure drop from original pressure P_1 , P_2

could be determined in this way. Eventually, water permeability for each specimen can be calculated under given conditions as in Table 3.

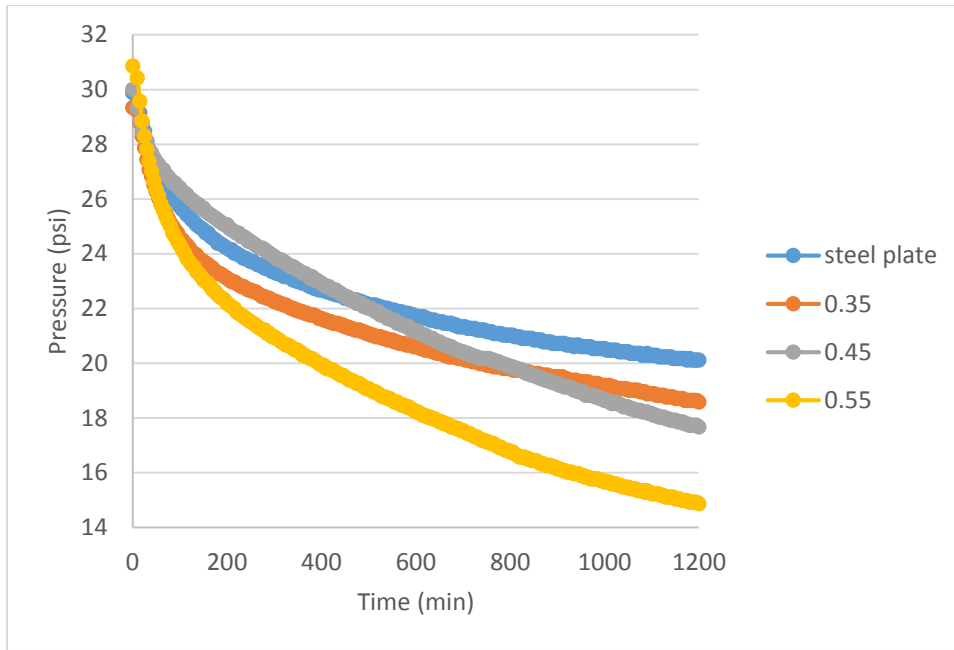


Figure 10. Tests with air saturated water at 70°F (selected data)

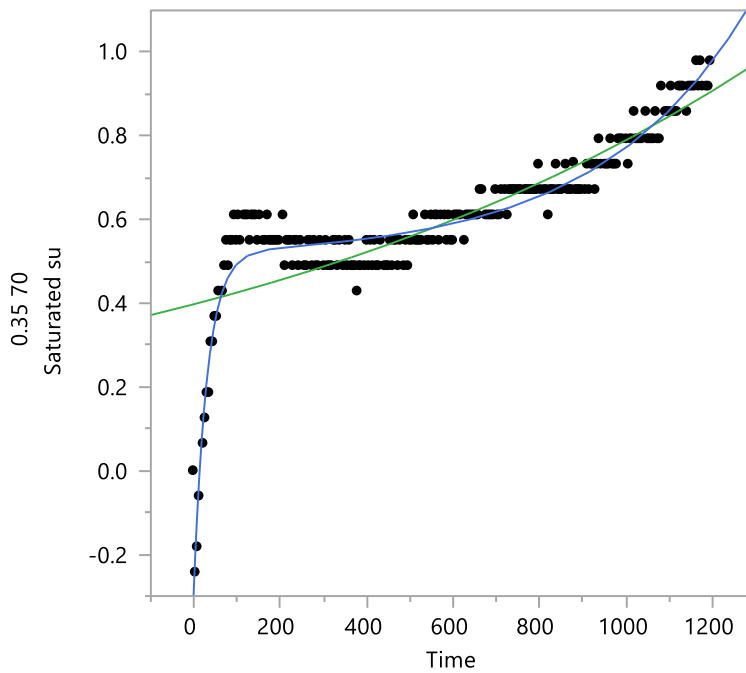


Figure 11. Absolute pressure drop for w/c=0.35 with air saturated water at 70°F

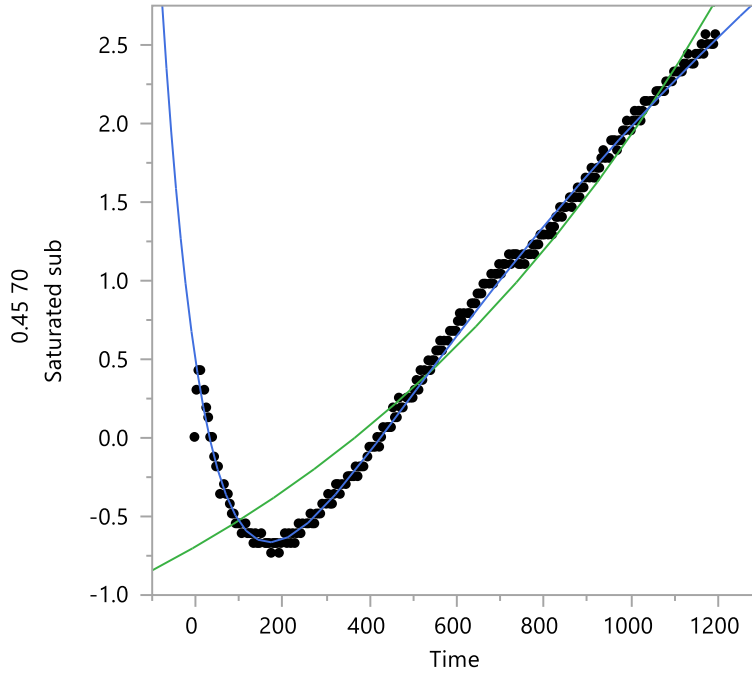


Figure 12. Absolute pressure drop for $w/c=0.45$ with air saturated water at 70°F

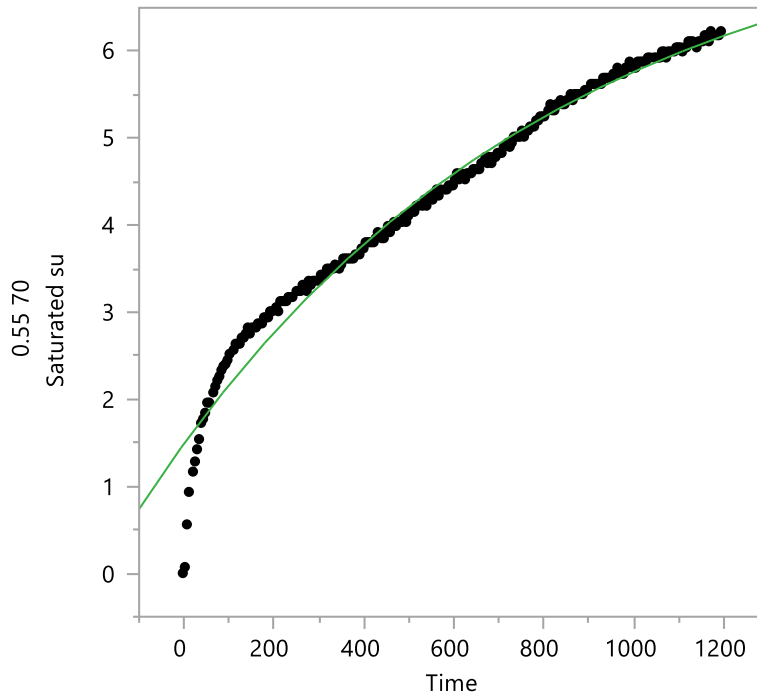


Figure 13. Absolute pressure drop for $w/c=0.55$ with air saturated water at 70°F

Table 3. Permeability for test samples at 70°F with air saturated water

w/c ratio	P1 (psi)	V1(ml)	P2 (psi)	V2(ml)	L, Thickness (cm)	t, Time (s)	K, Permeability (cm/s)
0.35	29.34	10	28.36	10.34	2.30	72000	3.42E-11
0.45	30.01	10	27.44	10.93	2.26	72000	9.15E-11
0.55	30.86	10	24.63	12.53	2.78	72000	3.15E-10

4.5 Conclusions

The following conclusions can be drawn from the present study:

- A newly developed water permeability test device is simple, cheap and easy to operate. The test measures the pressure drop within certain time period for a given sample. However, the test results are not reliable at this point.
- The major factors affecting test results include sealing of the system, temperature, and initial air volume.
- Test results of cement paste samples indicate that the “true” pressure drop (the difference between pressure of a sample and the pressure of steel plate) increasing with time. The rate of the pressure drop becomes constant after certain time.

- The permeability of cement paste can be calculated based on the pressure drop measured, which increases with water-to-cement ratio.
- Further refinement is needed to obtain consistent test results for given samples and test conditions.

References

- [1] T.C. Powers, H.M. Mann, L.E. Copeland, "The Flow of Water in Hardened Portland Cement Paste," *Highway Research Board Special Report*, July 1959.
- [2] P. Kumar Mehta, Paulo J.M. Monteiro, *Concrete Microstructure, Properties, and Materials*, McGraw-Hill, 2006, p. 140.
- [3] "Standard Test Method for Electrical Indication of Concrete's Ability to Resist Chloride Ion Penetration".*ASTM C1202*.

List of Figures

Figure 1. Flow rate vs. pressure for porous media with different permeability.....	39
Figure 2. Horizontal rotator	41
Figure 3. High shear mixer	41
Figure 4. Permeameter submerged in water	45
Figure 5. Effect of temperature on permeability measurement (steel plate).....	46
Figure 6. Effect of initial air volume on permeability measurement (at 70°F, steel plate).....	47
Figure 7. Effect of air saturation on permeability measurement (steel plate).....	48
Figure 8. Effect of repeatability on permeability measurement with air saturated water at 70°F (steel plate)	48
Figure 9. Effect of repeatability on permeability measurement for cement paste of water-to-cement ratio=0.35 with air saturated water at 70°F.....	49
Figure 10. Tests with air saturated water at 70°F (selected data)	51
Figure 11. Absolute pressure drop for w/c=0.35 with air saturated water at 70°F	51
Figure 12. Absolute pressure drop for w/c=0.45 with air saturated water at 70°F	52
Figure 13. Absolute pressure drop for w/c=0.55 with air saturated water at 70°F	52

List of Tables

Table 1. Mix proportions	42
Table 2. Parameters for Water Permeability Calculation	49
Table 3. Permeability for test samples at 70°F with air saturated water.....	53

CHAPTER V. CONCLUSIONS

The aim of this study is to identify the safe travel distance of water in capillary pores during freezing, which helps to prevent frost damage of cement paste. Safe travel distance is influenced by several factors and each factor plays a different role. Using the sensitivity study, conclusions can be drawn. Besides, water permeability is one of the major factors affecting the spacing factor for air voids. The development of low cost water permeameter is the experimental way to investigate water permeability for cement paste. Although there are some drawbacks for this apparatus, with further design improvements, it will measure properly for the water permeability of cement paste.

The main conclusions and recommendations are summarized as follows:

Paper one

- The maximum spacing factor should be around 210um for maximum pore pressure of 650psi (consistent with the values proposed by Powers in 1949). The pore pressure increases with increased spacing factor.
- For given $\eta=1.787$ Ns/m², $r_b=100\mu\text{m}$, $K=1.6*10^{-11}\text{cm/s}$, $d_wf/dt=0.25\text{m}^3/\text{m}^3*\text{s}$, $\bar{L}=210\mu\text{m}$, the maximum pore pressure reaches 650psi when effective degree of saturation is 0.92. The pore pressure increases with increased degree of saturation.
- For given $\eta=1.787$ Ns/m², $r_b=100\mu\text{m}$, $K=1.6*10^{-11}\text{cm/s}$, $S_f=0.92$, $\bar{L}=210\mu\text{m}$, the maximum pore pressure reaches 650psi when rate of ice formation is $0.25\text{m}^3/\text{m}^3*\text{s}$. The pore pressure increases with increased rate of ice formation.

- For given $\eta=1.787 \text{ Ns/m}^2$, $r_b=100\mu\text{m}$, $S_f =0.92$, $d_wf/dt=0.25\text{m}^3/\text{m}^3*\text{s}$, $\bar{L}=210\mu\text{m}$, the maximum pore pressure reaches 650psi when permeability is $1.6*10^{-11}\text{cm/s}$. The pore pressure increases with decreased permeability.
- Spacing factor requirement for F-T resistance ($P < 650\text{psi}$) frost may vary depends upon degree of saturation, rate of ice formation, and permeability.


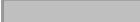


Paper two

- A newly developed water permeability test device is simple, cheap and easy to operate. The test measures the pressure drop within certain time period for a given sample. However, the test results are not reliable at this point.
- The major factors affecting test results include sealing of the system, temperature, and initial air volume.
- Test results of cement paste samples indicate that the “true” pressure drop (the difference between pressure of a sample and the pressure of steel plate) increasing with time. The rate of the pressure drop becomes constant after certain time.
- The permeability of cement paste can be calculated based on the pressure drop measured, which increases with water-to-cement ratio.
- Further refinement is needed to obtain consistent test results for given samples and test conditions.

APPENDIX A. STATISTIC ANALYSIS FOR WATER PERMEABILITY

ESTIMATION

Cement paste with w/c=0.35**Fit Curve****Model Comparison**

Model		AICc	AICc Weight	Weights	BIC
Biexponential 5P		-775.5386	1		-755.0153
Exponential 3P		-428.9763	5.558e-76		-415.2239
Model	SSE	MSE	RMSE	R-Square	
Biexponential 5P	0.5272127	0.0022435	0.0473652	0.9286533	
Exponential 3P	2.2734947	0.0095928	0.0979429	0.692332	

Exponential 3P**Prediction Model**

$$a + b * \text{Exp} \left[c * \text{Time} \right]$$

a = Asymptote

b = Scale

c = Growth Rate

Summary of Fit

AICc	-428.9763
BIC	-415.2239
SSE	2.2734947
MSE	0.0095928
RMSE	0.0979429
R-Square	0.692332

Parameter Estimates

Parameter	Estimate	Std Error	Lower 95%	Upper 95%
Asymptote	0.0194802	0.2371033	-0.445234	0.4841942
Scale	0.3782897	0.2234184	-0.059602	0.8161817
Growth Rate	0.0007111	0.0002844	0.0001538	0.0012684

Biexponential 5P**Prediction Model**

$$a + b * \text{Exp} \left[-c * \text{Time} \right] + d * \text{Exp} \left[-f * \text{Time} \right]$$

a = Asymptote

b = Scale 1

c = Decay Rate 1

d = Scale 2

f = Decay Rate 2


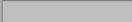


Summary of Fit

AICc	-775.5386
BIC	-755.0153
SSE	0.5272127
MSE	0.0022435
RMSE	0.0473652
R-Square	0.9286533

Parameter Estimates

Parameter	Estimate	Std Error	Lower 95%	Upper 95%
Asymptote	0.5078264	0.011427	0.4854299	0.5302228
Scale 1	0.0145421	0.0041633	0.0063822	0.0227019
Decay Rate 1	-0.002898	0.0002366	-0.003362	-0.002434
Scale 2	-0.792568	0.0326881	-0.856635	-0.7285
Decay Rate 2	0.0319839	0.0022683	0.0275381	0.0364297

Cement paste with w/c=0.45**Fit Curve****Model Comparison**

Model		AICc	AICc Weight	Weights	BIC
Biexponential 5P		-658.9688	1		-638.4455
Exponential 3P		10.571819	4.08e-146		24.324162
Model	SSE	MSE	RMSE	R-Square	
Biexponential 5P	0.8568918	0.0036463	0.060385	0.9966135	
Exponential 3P	14.193279	0.0598873	0.2447187	0.9439072	

Exponential 3P**Prediction Model**

$$a + b * \text{Exp} \left[c * \text{Time} \right]$$

a = Asymptote

b = Scale

c = Growth Rate

Summary of Fit

AICc	10.571819
BIC	24.324162
SSE	14.193279
MSE	0.0598873
RMSE	0.2447187
R-Square	0.9439072

Parameter Estimates

Parameter	Estimate	Std Error	Lower 95%	Upper 95%
Asymptote	-2.410311	0.3542869	-3.104701	-1.715922
Scale	1.7191751	0.3205095	1.0909881	2.3473622
Growth Rate	0.0009252	0.0001052	0.000719	0.0011314

Biexponential 5P**Prediction Model**

$$a + b * \text{Exp} \left[-c * \text{Time} \right] + d * \text{Exp} \left[-f * \text{Time} \right]$$

a = Asymptote

b = Scale 1

c = Decay Rate 1

d = Scale 2

f = Decay Rate 2

Summary of Fit

AICc	-658.9688
BIC	-638.4455
SSE	0.8568918
MSE	0.0036463
RMSE	0.060385
R-Square	0.9966135

Parameter Estimates

Parameter	Estimate	Std Error	Lower 95%	Upper 95%
Asymptote	7.5871012	0.6942742	6.2263488	8.9478536
Scale 1	-9.574478	0.6176893	-10.78513	-8.363829
Decay Rate 1	0.0005349	5.9456e-5	0.0004184	0.0006515
Scale 2	2.474234	0.0743302	2.3285494	2.6199186
Decay Rate 2	0.0095175	0.0004304	0.008674	0.0103611

Cement paste with w/c=0.55

Fit Curve

Model Comparison

Model		AICc	BIC	SSE	MSE
Exponential 3P	—	-64.1656	-50.41325	10.395392	0.0438624
Model	RMSE	R-Square			
Exponential 3P	0.2094336	0.9763389			

Exponential 3P

Prediction Model

$$a + b * \text{Exp} \left[c * \text{Time} \right]$$

a = Asymptote

b = Scale

c = Growth Rate

Summary of Fit

AICc	-64.1656
BIC	-50.41325
SSE	10.395392
MSE	0.0438624
RMSE	0.2094336
R-Square	0.9763389

Parameter Estimates

Parameter	Estimate	Std Error	Lower 95%	Upper 95%
Asymptote	7.8197703	0.2082381	7.4116311	8.2279095
Scale	-6.328191	0.1826993	-6.686275	-5.970107
Growth Rate	-0.001125	6.8084e-5	-0.001258	-0.000991

APPENDIX B. VIEWS OF WATER PERMEAMETER

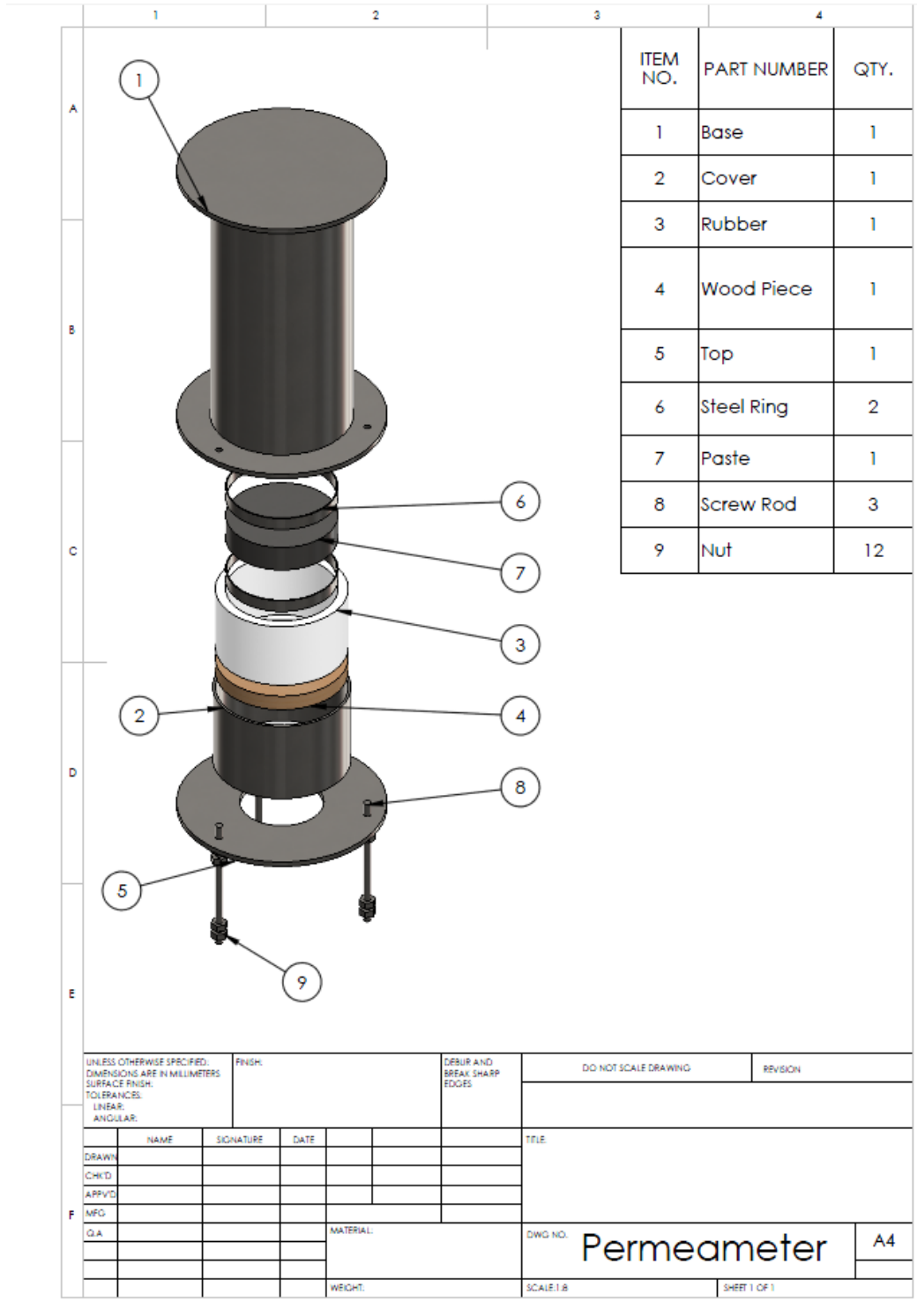


Figure B1. Details of water permeameter

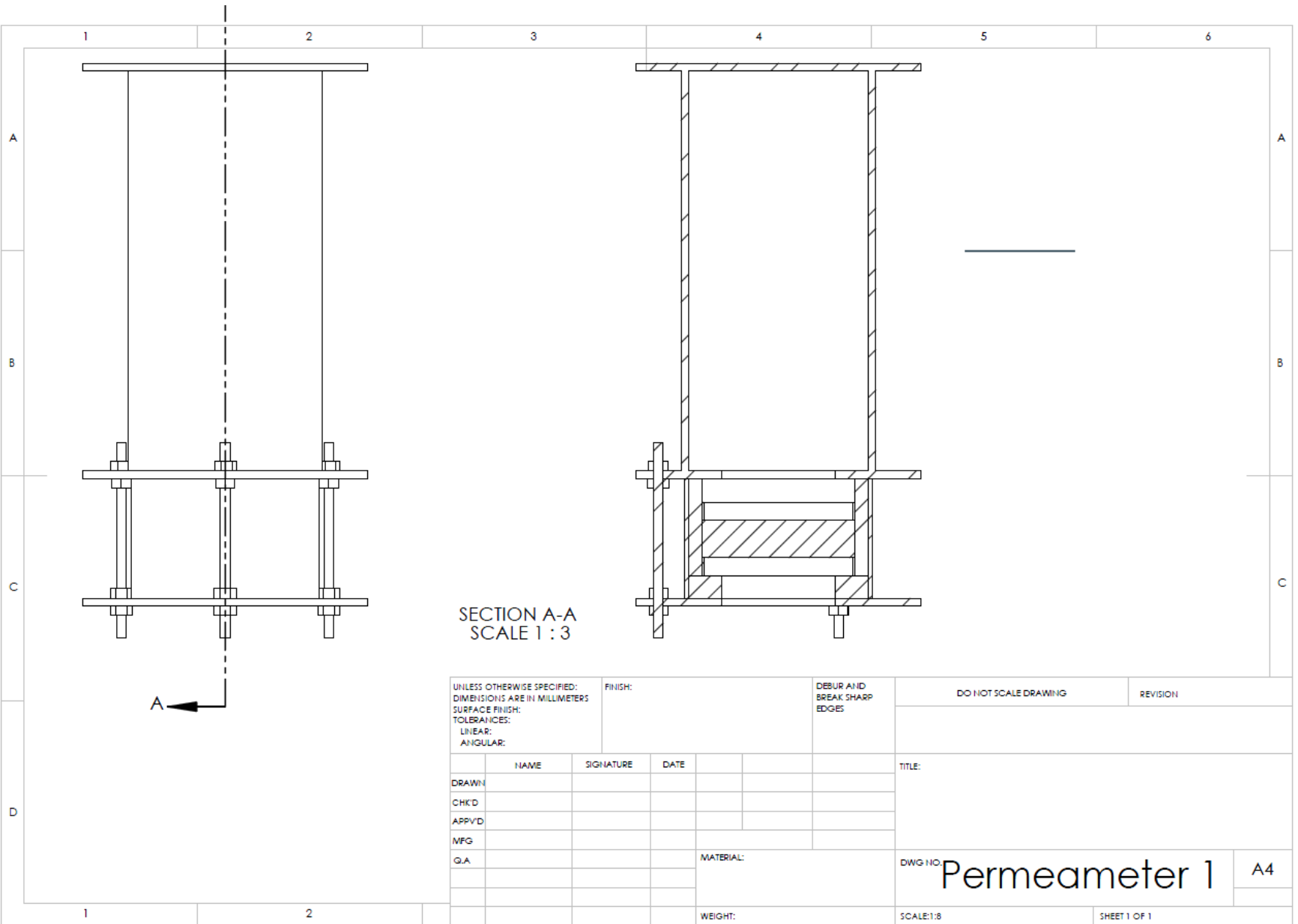


Figure B2. Front view for water permeameter

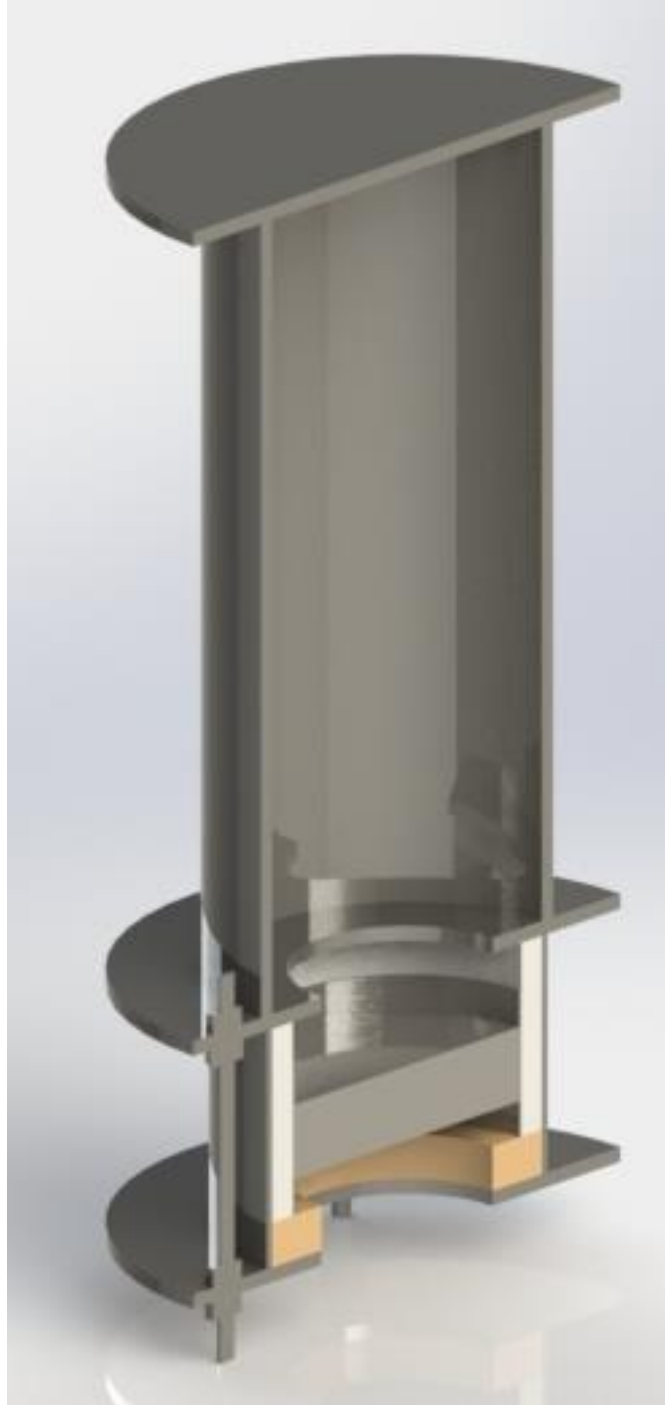


Figure B3. Cut section view for water permeameter



Figure B4. Water permeameter after revision